

The Efficacy of Utilizing X-Ray Fluorescence Techniques in Quantifying Accumulation Rates of  
Trapped Material in Coral Cores from Belize

By  
Conner Kingsley  
University of Colorado at Boulder

A thesis submitted to the  
University of Colorado at Boulder  
In partial fulfillment  
Of the requirements to receive  
Honors designation in  
Environmental Studies  
May 2018

Thesis Advisors:

*Atreyee Bhattacharya*, Environmental Studies, Committee Chair

*Dale Miller*, Environmental Studies

*Heidi Souder*, Baker RAP

## ABSTRACT

Caribbean coral reefs are some of the most threatened marine ecosystems in the world. Predictions have a 90% mortality of coral reefs by 2050; right now, over 50% of coral reefs have died. Research suggests that environmental stressors of local origin, such as sediment run off, can reduce the resilience of these reefs to global threats i.e. ocean warming. Sedimentation can stunt coral growth and reduce its resilience; trapped material could render coral skeletons brittle. Despite the importance of quantifying sources and types of materials trapped in corals, the research community is yet to develop techniques that allow accurate representation of trapped matter.

The dataset presented here explores the usefulness of X-Ray Fluorescence (XRF), a non-destructive x-ray scanning technique – to estimate metal content in coral cores collected from four locations near Belize. The coral cores together cover a period of 1876-2006. Substituted metal content (not trapped metal content) from these cores has been well-studied using solution-based Inductively Coupled Plasma Mass Spectrometer (ICP-MS), which provided us the opportunity to test the efficacy of the XRF technique by correlating our results to the ICP-MS results.

The XRF technique is a viable supplement in determining trapped metal content in coral cores. It may be particularly helpful for assessing resistant phases such as grains of sediment that are not fully dissolved in the typical solution-based ICP-MS methodology. XRF should be used in association with the ICP-MS methods for a full characterization of elemental abundance in coral skeletons. Our research has strong implications far beyond that of these corals. It establishes XRF scanning as a viable methodology to characterize trapped content that will assist researchers to more fully assess the causes and impacts of local stressors on coral reefs.

## **PREFACE**

I would like to thank my advisor, Atreyee Bhattacharya, with whom I have worked with over the past three years and has given me the confidence and the ability to understand all of this scientific research. I would also like to thank Alexis Urbalejo who has been by my side during this entire project. I would like to thank Alex Hangsterfer for allowing us to use the X-Ray Fluorescence at Scripps Institute of Oceanography. I would also like to thank Jessica Carilli for sharing her samples and for allowing us to build upon her impressive work. I would like to thank Dale Miller for helping me to write this Honors Thesis and for meeting with me week after week. And finally, I would like to thank Heidi Souder for her help in getting this project done. I hope this honors thesis offers a new glimpse into the usefulness of corals as proxy tools. I hope scientists can uncover more uses for X-Ray Fluorescence in coral studies with the work we have done here.

## TABLE OF CONTENTS

Introduction .....	Page 1
Background .....	Page 4
Study Location .....	Page 7
Methodology .....	Page 10
Results .....	Page 21
Discussions and Conclusions.....	Page 35
Recommendation for Future Work in Coral Studies.....	Page 42
Bibliography .....	Page 43

## INTRODUCTION

The Mesoamerican coral reefs are home to some of the most diverse ecosystems in the world, yet they are also the most threatened. Threats to this reef ecosystem are both global in nature (ocean acidification, warming ocean temperatures, etc.) as well as local e.g. increased runoff (agriculture, mining) and exploitative fishing (such practices often remove key fish species that in turn upset the nutrient balance in coral ecosystems). Local threats, such as sediment runoff (from agriculture, beach construction, and mining upstream of rivers that drain into the regions) can reduce resilience of the reef-building coral species to global threats, making the reefs vulnerable to the effects of global stressors e.g. increased risk of bleaching. In addition, sedimentation is a stressor that can increase the amount of particulate matter in the water column, thereby affecting the amount taken up by coral.

Zooxanthellae living on the corals can consume these metals from sedimentation and incorporate them into the calcium carbonate structure i.e.  $\text{CaAl}$ ,  $\text{CaFe}$ , etc.: we call these substituted metals within the coral skeletons. However, when polyps are damaged or destroyed, cavities are formed in which metals in the water column can enter the coral skeleton and become trapped in the coral lattice. Trace (metals normally present in animal and plants cells), major (Si, Ti, Al, Fe, Mn, Mg, Ca, Na, K, P), and minor (in abundances of  $>1$  ppm: Ba, Ce, Co, Cr, Cu, etc.) content of substituted metal in the skeletal material in these cores have been well studied using solution-based Inductively Coupled Plasma Mass Spectrometry (ICP-MS). ICP-MS involves dissolving subsamples of coral skeletons to measure elemental content and as such, measures purely substituted metal within the coral lattice. This method has allowed researchers to understand heavy runoff from local sources such as agricultural and industrial activities from watersheds surrounding the Mesoamerican Reef.

The first method in which metals infiltrate the coral lattice is through this direct substitution in the skeleton, which is measured by ICP-MS. The second method is when metals become purely trapped within the coral lattice. In this study, we focus on trapped metal.

Particulate matter can then become trapped inside cavities of coral skeletons (composed of calcium carbonate created by the coral polyps living on the corals) which can lead to reduced skeletal growth rates, reduced fecundity, and changes in community structure. Trapped material could render coral skeletons brittle, thereby making reefs more susceptible to physical damage from tourism (ships), dredging and wave action (associated with weather events that also might be affected by 21<sup>st</sup> century climate change). Furthermore, trapping of materials is a potential method by which metals accumulate in reef-building coral skeletons, which could potentially contribute to coral bleaching events. In addition, material trapped in coral skeletons can provide key information on the impact of sedimentation on calcification rates in corals. Previous studies in the Mesoamerican coral reefs have provided an understanding of the degree of substituted metal concentration in coral skeletons by utilizing the ICP-MS method. However, there is no method for estimating the amount and effects of purely trapped metal inside the coral lattice.

In this study, we explore the potential for a new method, X-Ray Fluorescence (XRF) (a tool widely used in environmental sciences but not in coral studies) to characterize and quantify trapped material within skeletal cavities in coral samples. XRF is a non-destructive x-ray scanning tool, which measures metal content for over fifty elements and is used for analyzing a wide range of specimens such as rocks, minerals, sediments, and fluids. XRF allows for relatively quick and easy sample preparation and scanning, with an average analysis time of around 12 hours. XRF is particularly useful for bulk analyses, i.e. measuring metal content. XRF is particularly well suited for analysis of major (Si, Ti, Al, Fe, Mn, Mg, Ca, Na, K, P), minor (in abundances of >1 ppm: Ba, Ce, Co, Cr, Cu, etc.), and trace elements. Virtually any solid or liquid material can be analyzed using XRF, making it a great candidate for coral studies.

We analyzed four coral slabs (samples cored from *Montastraea faveolata* coral species and sawed into flat slabs for relative ease of analysis) from four separate sites near Belize and Honduras. We used the XRF scanning technology to measure metal content in these four coral slabs. We compared the XRF data to existing ICP-MS data for metal content for the same four samples to determine if XRF is a viable tool for measuring trapped metal in reef building Mesoamerican coral. In the first part of this study we focused on comparing XRF measurements to ICP-MS measurements of elemental accumulations of 6 metals (Barium, Chromium, Copper,

Manganese, Lead, and Zinc) in the same four coral samples. By comparing XRF data to ICP-MS data (which measures purely substituted metals in the  $\text{CaCO}_3$ , not trapped metal, by dissolving subsamples of annual segments of the coral skeleton) we were able to determine whether or not the XRF method measured purely substituted metal. In the second part of this study we used linear regression analysis to determine if any of the resistant metals (elements that tend to not substitute within the coral lattice due to their size) measured by XRF accumulated at similar rates within the coral skeleton. The elements that are most likely to become purely trapped in the coral lattice are Zircon, Titanium, Aluminum, and Iron. Zircon and Titanium are purely trapped within the coral skeleton, while Aluminum and Iron can be either substituted or trapped. We found significant correlation ( $>.7$ ) between resistant phases.

Due to the high correlation of these resistant metals from the XRF measurements, we determined that XRF measurements assess elemental abundances of trapped material. We conclude that the non-destructive XRF technique is a viable method to characterize materials trapped in coral cores. XRF cannot estimate trace quantities of elements substituted in the  $\text{CaCO}_3$  of coral skeletons, possibly because the XRF technique can only estimate discrete mineral assemblages. XRF will assist scientists in measuring trapped metal in addition to measuring substituted metal with ICP-MS. This will allow for a better understanding of the cause and effects of sedimentation on coral reefs. We find that XRF offers a viable methodology to characterize and quantify trapped material, especially resistant phases of minerals that are common sourced from weathered material and persevere in the ocean waters.

## BACKGROUND

There are two methods by which materials, and by extension, metals, become incorporated into coral skeletons: (a) accumulation of particles in coral cavities (Barnard et al., 1974) in which no chemical reaction occurs and (b) substitution of metal in the  $\text{CaCO}_3$  lattice – a process that is temperature dependent and in which a chemical reaction occurs (Sinclair et al, 1998). There is currently one method already being utilized in coral studies for understanding metal accumulation and that is Inductively Coupled Plasma Mass Spectrometry (ICP-MS) (Sinclair et al. 1998). ICP-MS is where freshly broken coral samples are dissolved in a solution of concentrated nitric and hydrofluoric acid and 6N nitric acid (Carilli et al 2009). The elemental abundances in the solution are then measured using Inductively Coupled Plasma (ICP), in which the solutions are heated to extreme levels (around 6000-10000 degrees Kelvin) (Prouty et al. 2008) which converts the compounds in the solution into atoms, and then, into ions. The ions are separated according to their mass and are measured by the Mass Spectrometer, which provides an estimate of the abundance of elements within the sample solution and by inference in the original samples (in this case it would be coral skeletons). The ICP-MS method has been used to measure elemental abundances and to understand metal accumulation in coral skeleton; however, the method only measures elements/metals substituted in the calcium carbonate, which only partly makes up the detrital matter in the skeletal matrix (Xuefei et al 2015, Sinclair et al, 1998).

In fact, most of our understanding of trapped material in coral skeletons is derived from a study conducted by Barnard et al. (1974); in this study, the authors describe how they found materials trapped within the cavities of coral skeleton. Furthermore, Barnard et al. (1974) reported that coral polyps are normally able to reject (slough) particulate matter. However, when polyps are damaged or destroyed, particulate material, sourced from weathered soil, can enter the skeletal cavities; the particles become sealed into the skeleton after the polyp regenerates or recovers (Figure 1). The “incorporation of particulates in the skeletal material tends to be random and erratic (Goreau 1977) and some hypothesize that “undamaged corals have less chance of collecting particulates” (Brown & Molly 1982, Barnes 200).



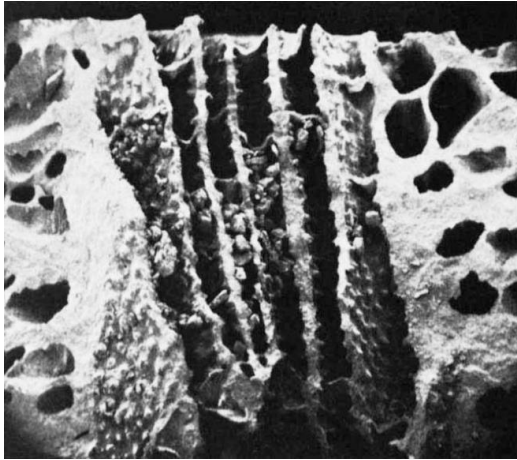


**Figure 1: Detrital material trapped in corallite of *Soenastrea hyades* from North Carolina.** This is a microscopic examination of freshly broken surfaces etched with acid. It reveals skeletal cavities which had been capped with dissepiment after being partially filled with detrital material. The damage and then particle accumulation are because of trapped material. (from Barnard et al., 1974)

The Barnard et al. (1974) study indicates that as corals grow they may preserve a continuous record of non-carbonate sediments, that were suspended in the waters around them, in their skeletons. Barnard suggests that these non-carbonate sediments become preserved in the coral skeleton in two different ways. Material may become purely “trapped” within the skeleton and may also become substituted, in which “non carbonate material is embedded in the skeletal carbonate matrix.” Most studies to date only rely on analysis of the substituted form of non-carbonate sediments within the coral skeleton. Thus, “previous elemental chemical analyses must be interpreted with caution in cases in which the presence of trapped terrigenous detritus was not noted” (Barnard et al. 1974).

The effects of trapped material vary according to types of coral reefs, size, frequency, clearing ability, colony morphology, and species resistance (Bak and Elgershuizen 1976, Dodge and Lang 1983, Rice and Hunter 1992, Stafford-Smith and Ormond 1992, Bastidas et al. 1999). Metal incorporation, as a result of sedimentation, appears to have detrimental effects on the structure of coral reef communities such as brittleness and increased occurrences of bleaching events (Bastidas et al. 1999). Irritation, damage, or destruction of the polyps may open up more cavities in the coral skeleton and therefore lead to even more detrital matter becoming preserved in the coral skeleton. This in turn could lead to even more polyps becoming destroyed, leading to more bleaching events.

Clearly, it is important to understand the effects of particulate accumulation. Currently there are no proven methods to help scientists understand the amount of trapped metal within the coral lattice. In this study, we use X-Ray Fluorescence (XRF) to determine the proportion of trapped metal, versus purely substituted metal, within coral samples. We chose XRF because it is a quick, low cost, and non-destructive technique that may shed light on purely trapped metals within the coral skeleton. XRF is a tool commonly used in environmental studies, mainly to study sediment cores due to its superiority in measuring major and minor metals, but has not been used to study coral cores. Mainly the environmental community has not utilized XRF because coral samples are highly random and are difficult to study due to the high variability of growth bands. In this study, we devise a method for XRF to overcome these variabilities and provide a viable technique for measuring metal content in coral samples.

## STUDY LOCATION

The coral ‘cores’ used in this study are samples drilled from the *Montastraea faveolata* hermatypic corals in the Mesoamerican reefs. Samples were taken from the Mesoamerican coral reef from the Turneffe Atoll (HMF), Sapodila Cayas (SMF), Utila (UMF), and Cayos Cochinos (CMF) (figure 3). We used samples from T1, not T2, however. Figure 2 shows the four sites, HMF is off the east coast of Belize, SMF is near the Gulf of Honduras (which experiences the most land erosion), UMF and CMF are north of Honduras. Freshwater runoff has doubled and there has been a 20-fold increase in the amount of sediment eroded due to land use changes in the watersheds surrounding these Mesoamerican reef sites (Carilli et al. 2009). Figure 3 gives an account of the rainfall and soil erosion experienced by Belize and Honduras. Belize experiences less rainfall and sediment erosion than the Honduras sites, which point towards more pollutants in the water column and more uptake of detrital matter in corals at the SMF UMF, and CMF sites.

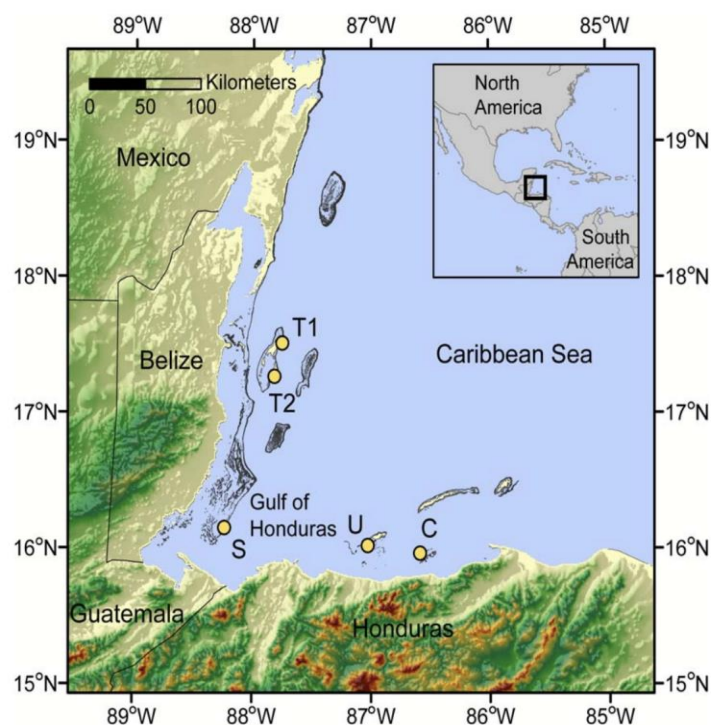


**Figure 2: Location of all four sites where coral cores used for this XRF study were cored.** Turneffe Atoll (HMF – we do not use T2 in our study), Sapodilla Cayas (SMF), Utila (UMF), and Cayos Cochinos (CMF) surrounding land shows topography, with greens and warm colors higher than tan coloring (image from Carilli et al. 2009) These are the sites where our coral slabs are from and of which are measured by XRF. The sites and areas around these coral reefs have been studied in depth especially by Carilli et al. 2009 and Burk and Sugg 2006. These studies have determined relative amounts of discharge coming from rivers and other water sources and are described in the figures below.

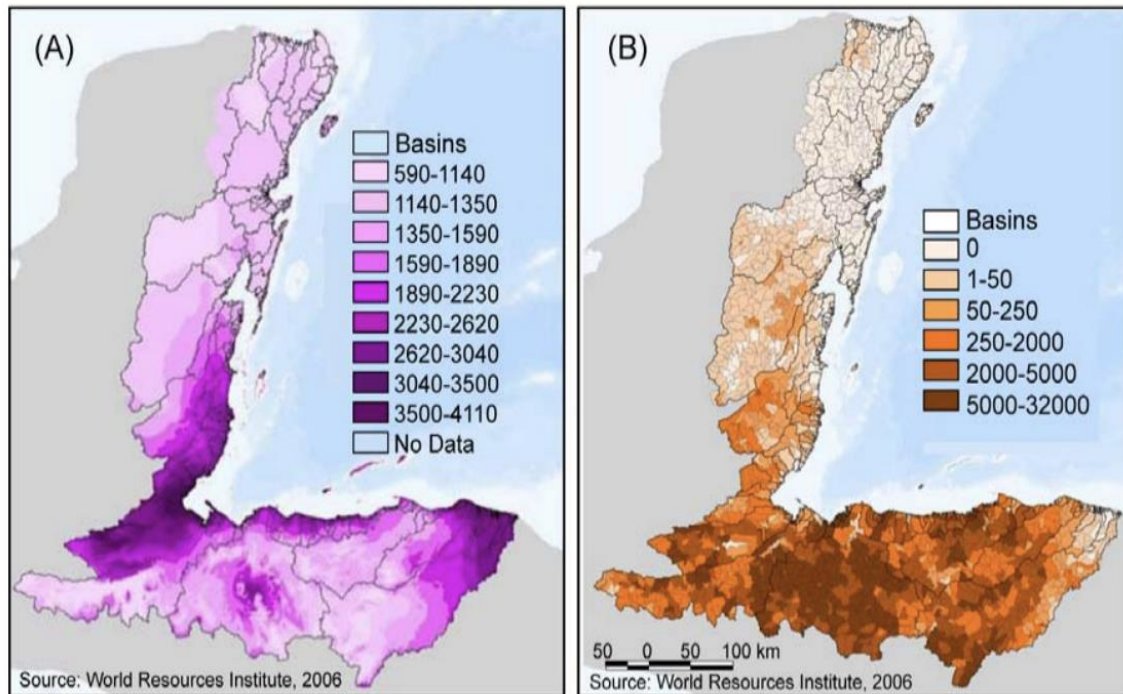


**Figure 3: Watersheds draining onto the MesoAmerican reef with: (A) annual rainfall in mm and (B) annual sediment erosion in meters/km<sup>2</sup>.** This gives us a relative understanding of the types of sedimentation and pollution coming from the coasts and of which could potentially be affecting the coral reefs off the coast of Belize. These images were altered by Carilli et al. 2009 and are originally from Burk and Sugg 2006.

However, the sites were chosen because of different degrees of coastal influence. CMF is the most polluted site, UMF is second, SMF is third, and HMF is the least polluted site. Jessica Carilli collected cores from these four sites using a 5-cm diameter stainless steel and brass core barrel with carbide cutting teeth driven by a reversible air powered drill. Coral tissues were removed using a water-pik and then the cores were rinsed with freshwater and air dried. An 8mm slab was then removed from the middle of each core using a carbide-tipped double bladed table saw lubricated with fresh water for relative ease of analysis. (Carilli et al. 2009). Table 1 describes the exact coordinates where Jessica Carilli took these coral samples.

Environmental indicators accumulate within the growth bands of calcium carbonate each year. Detrital matter that is within the water column accumulates within each of these growth bands.

By studying ‘slabs’ from coral reefs we can estimate the amount of particulate matter that accumulated within the coral each year and therefore, gain a picture of the climactic and environmental history of the waters surrounding the coral samples. This same process is also described in an animation put together by myself and Alexis Urbalejo ([link](#)).

We scanned the four coral slabs – each slab representing a site near the coast of Belize, about 120cm representing on an average 100 years of continuous growth – using XRF.

**Table 1 - Coral core selection site locations** This gives the four sites we used their dive site name, the coordinates where the coral cores were taken, we do not use the coordinates in our study, but it gives a good reference as to where the cores were taken from.

Site	Dive Site Name	Coordinates
Turneffe	Dog's Head Caye	17°29'59"N, 87°45'30"W
Sapodilla	Frank's Caye, NE Buoy	16°07'45"N, 88°14'59"W
Utila	Diamond Caye	16°03'52"N, 86°57'30"W
Cayos Cohinos	Pelican Point, Peli	15°58'41"N, 86°29'06"W

## METHODOLOGY

The main focus of this study, the X-Ray Fluorescence (XRF) tool (figure 4), measures proportions for over fifty different elements by subjecting samples to different strengths of x-rays (10kv, 30kv, and 50kv) to measure trapped metal content without harming the coral samples.



**Figure 4: Photo of Avaatech XRF Core Scanner (taken from [avaatech.com](http://avaatech.com))**

The x-rays force atoms present in the sample to ionize: an increase in energy from the x-ray forces electrons in each element to be ejected or expelled to an outer (higher energy) shell from an inner (lower energy) shell (typically K and L electron shells). The ejected electron leaves a “hole” in the structure of the atom making it unstable. This ‘hole’ is then filled by electrons from an outer layer. The process of electrons jumping to different energy levels is called fluorescence (figure 5).

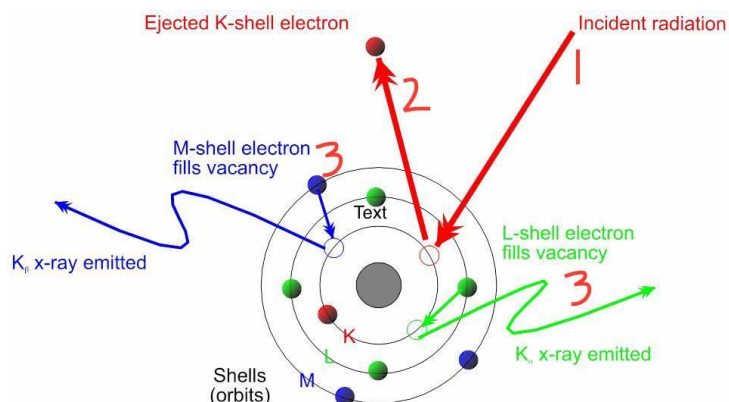


**Figure 5: How XRF works at the atomic level (Bruker 2017)**

1. X-Ray is emitted by XRF
2. Electron is dispelled
3. Electron from higher energy level moves to lower energy level and emits characteristic X-Ray Photons

The binding energy, which is emitted via characteristic x-ray photons once an electron jumps from an orbital shell, is dependent on the distance of these electrons from the nucleus of the atom. The electron loses some of this energy when it moves from one high level to a low level, due to the fluorescence. The loss of energy emitted is equivalent to the distance between the two “orbital shells”. XRF identifies these different emitted energy jumps via a Wavelength Dispersive Spectrometer (WDS). It then determines the amount of these elements by calculating the proportion in which the individual energies appear. Each element has its own distinct fluorescence, which helps to identify the element. The degree of fluorescence is proportional to the abundance in which the element occurs within the sample.

XRF has been effective for the study of elemental abundances and variations in sediment cores and rock samples in environmental sciences – it offers a way for scientists to study the “typical disordered, heterogeneous, and fragile samples” (Gao 2006). The non-destructive, quick, and low cost scanning features that XRF offers make it a phenomenal and extremely powerful tool for environmental studies. XRF scans samples in less than 24 hours, it does not require any chemical analysis, and its only costs are from the electricity and upkeep. XRF has been commonly used in studying lakes cores and terrestrial samples, but not coral samples. Particularly, it has provided detailed palaeoenvironmental archives reflecting past climate, temperature, and vegetation by determining the past accumulation of metals and sediments within proxy data, such as sediment cores. Standard analytical methods for discrete sample analysis are discontinuous, time consuming, and expensive. (Rothwell and Croudace 2015). When XRF was invented it offered a

way for researchers studying sediment cores to almost instantly analyze their samples. For example, a major advantage of the Avaatech XRF (the one used in this study) was that it could even be containerized for sea-going, allowing acquisition of sediment records within a few hours of coring (Jansen et al. 1990). We decided that these features are ideally suited not just for sediment cores but also for coral cores. A scanning technique that simply takes measurements every 2mm along the slab seems, in theory, to be not applicable to the high variability of growth bands in coral cores. However, with a proper analysis and breakdown of the XRF data we determined that XRF could be an extremely useful tool for measuring trapped metal in coral samples.

The XRF scanned each coral sample in 12-13 hours at three different strengths: 10 kilovolts, 30 kilovolts, and 50 kilovolts. Each x-ray strength determines the amount of different metals. 10 kilovolts measures the amounts of Al, Si, P, S, Cl, K, Ca, Ti, Cr, Mn, Fe, and Rh. 30 kilovolts measures the amounts of Cu, Zn, Ga, Br, Rb, Sr, Y, Zr, Nb, Mo, Pb, and Bi. 50 kilovolts measures the amounts of Ag, Cd, Sn, Te, and Ba. The Avaatech XRF (model of XRF used at Scripps Institute of Oceanography, operated by Alex Hangsterfer) sends three excel files (10kv, 30kv, 50kv) with measurements for the accumulation of each metal within the sample to a desktop computer. All three excel files were combined into one file. We then spliced data where the XRF did not measure metal content on the coral slabs i.e. spaces between pieces of coral slabs (figures 8-11). XRF measures these spaces regardless, so when the data drops off to near zero, those measurements must be spliced. When the data showed XRF was measuring spots without any coral, significantly different numbers from the previous measurements appeared. We took extreme precaution to delete this data.

The XRF was set to a resolution of 2mm i.e. it took measurements every 2mm along the coral slab. We then correlated these measurements to the years in which they accumulated in the coral skeleton by creating age models for each coral sample. We divided each year's extension rates (table 2) by 2mm (every XRF point) to show the number of XRF measurements made for each year's growth band on the coral sample. However, each XRF point measures only a sample of metal accumulation, not the total amount of metal across the entire sample. In addition, each growth band will generally take 1-5 XRF points to measure its entirety. To account for this we



averaged the XRF measurements within each growth band to get a representative amount of metal accumulation within each growth band i.e. for each year. Averaging the metal content gave us a better understanding of the accumulation of metal for each year in the coral skeleton. This gave us the annual average accumulation for each of the fifty metals. We then created ratios for the annual average accumulation of each metal against the annual average amount of calcium. Since corals are made of calcium carbonate this gave us a better understanding of the proportion of metal against calcium (which makes up most of the coral).

**Table 2: Example of Carilli's work on extension length of UMF.** Includes density and calcification – though we only looked at extension lengths to correlate to our XRF data and the years. Calcification helped us to see the total amount in which the corals grew each year

Year	Extension	Density	Calcification
	cm	$\text{g/cm}^3$	Extension*Density
2005	.24	1.72	.41
2004	.24	1.72	.41
2003	.24	1.99	.45
2002	.18	2.31	.56
2001	.18	2.83	.49
2000	.14	2.83	.49

We chose the samples from the Mesoamerican coral reefs because previous analysis had been done on them with the Inductively Coupled Plasma Mass Spectrometer (ICP-MS) method. This allowed us to compare data for the XRF to the ICP-MS data to determine if the XRF method measures purely substituted metals in the coral skeleton. We then compared the XRF data for resistant metals (metals unlikely to become trapped within the coral lattice) to determine if XRF measures trapped metal.

The Mesoamerican coral reefs are home to some of the most diverse ecosystems in the world. Our coral samples offer extremely useful data about the environmental history of the water, nearby land erosions rates, and human impacts. Researchers typically take these “cores” (Figure 7) from hermatypic corals (figure 6) to study the past climate and environment. Each year zooxanthellae living in a symbiotic relationship with hermatypic corals provide corals with glucose, glycerol, and amino acids so the corals can produce layers of Calcium Carbonate. They build a new layer of Calcium Carbonate in the winter and in the summer. Corals incorporate detrital material from the water column into the calcium carbonate skeleton each year. Particularly, hermatypic corals (figure 6) are often used for understanding environmental history because they have round, wave-resistant structures, and have high rates of calcium carbonate production, which is highly desirable for creating coral slabs (Druffel 1997).

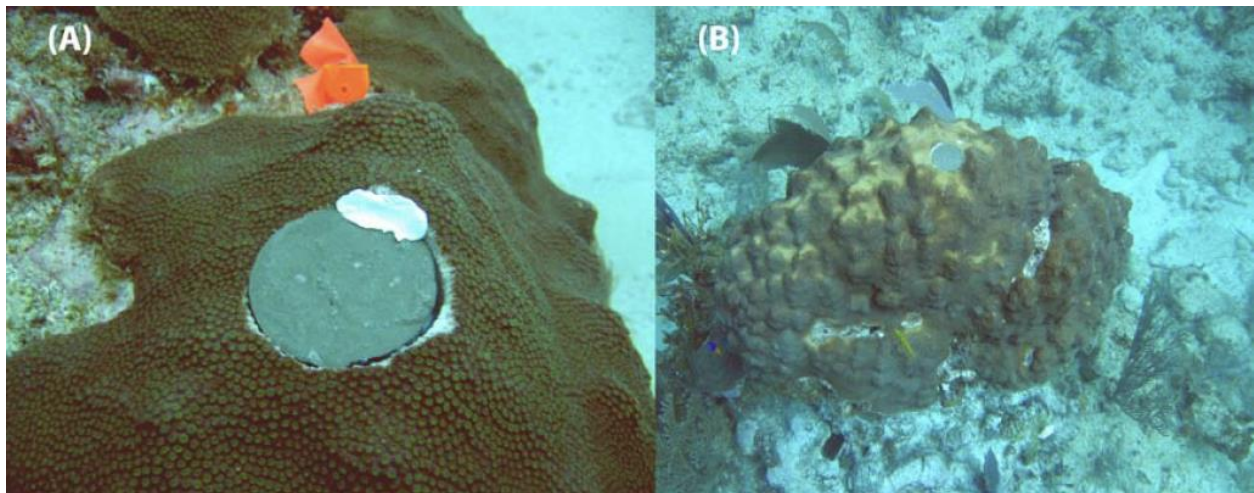


**Figure 6: Hermatypic corals from the Mesoamerican coral reefs.** (A) Is a completely healthy and functioning hermatypic coral, while (B) has slight paling due to a bleaching event.



**Figure 7: Drilling of coral cores from site in Belize.** Photo taken from Jessica Carilli.

In particular, corals are continuously calcifying and producing new density bands. The polyp in the coral, which contacts the skeleton of the coral via the ectoderm and hosts the zooxanthellae, secretes calcium carbonate, building “annual growth bands”. These growth bands are discernable by x-rays to show high density and low density bands. Higher density growth bands tend to be found during summer months, while less dense bands form during winter months (Hudson et al. 1994 and Glynn 1993). Together these bands consist of one calendar years’ worth of growth (figure 8). Researchers typically use chemical and physical parameters (including extension rates, changes in density, calcification – table 2) from the hermatypic corals to reconstruct the environmental history of the water, nearby land erosion rates, and human impacts. The coral slabs from the four sites are pictured in figures 9-12.

To gain a better understanding of the coral slabs we needed to determine the year in which each density band grew. Carilli determined the year which each density band grew by analyzing

digital x-rays of the coral slabs (figure 8) using the program Coral XDS (Helmle et al. 2002 and Carilli et al 30).

We use coral slabs from the four sites HMF, SMF, CMF, and UMF (Refer to Figure 2). Many of the coral slabs were broken into pieces due to their fragility. We define the section number of each coral slab by the positions of each piece in the photographs (figures 9-12).

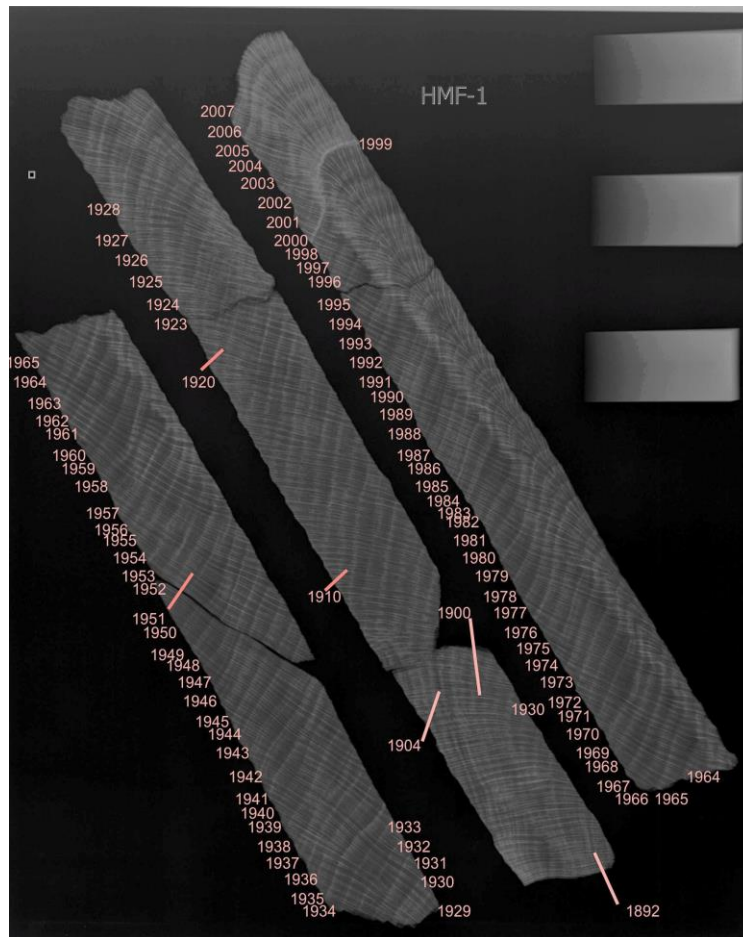


**Figure 8: X-Ray photo of HMF site coral slab with dating of each growth band determined by Carilli et al 2009.** Light bands correspond to summer months and dark bands correspond to winter months. Together they are on full calendar year of growth. HMF coral slab was drilled out of the coral from the years 1892-2005.



**Figure 9: Pictures of HMF Coral slab sections 1, 2, 3, 4, 5, 6, and 7 before scanning by XRF.** Sections 1-7 of HMF put together inside of the XRF before scanning. Sections 1&2 correspond to years 2005-1964, sections 3 & 4 correspond 1965-1929, and sections 5, 6, and 7 correspond to years 1928-1892. We do not account for the years before 1905 in the XRF study because other coral slabs did not go so far back. Section 1 is from 250cm-380, section 2 is from 380cm to 640cm, section 3 is from 640cm to 750/820cm, section 4 is from 750cm/820cm-950cm, section 5 is from 950cm to 1060cm, section 6 is from 1060cm to 1240cm, and section 7 is from 1240cm to 1365cm. The XRF took these pictures before it scanned them. Labelling on the cores helps us to determine where each part went so they were in the correct order.



**Figure 10: Pictures of SMF Coral slab sections 1, 2, 3, 4, 5, 6, 7, and 8 before scanning by XRF.** Sections 1-8 of the SMF coral slab inside of the XRF before scanning. Section 2 and 3 correspond to 2005-1972, section 4 corresponds to 1971-1962, section 5 corresponds to 1961-1952, section 6 corresponds to 1951-1940, section 7 corresponds to 1940-1917, and section 8 corresponds to 1916 to 1901. We do not account for 1901-1904 in our study since other slabs do not go that far back. Section 1 (which was not scanned by XRF) is from 125cm-162cm, section 2 is from 250cm-375cm, section 3 is from 375cm-500cm, section 4 is from 500cm-570cm, section 5 is from 570cm-655cm, section 6 is from 655cm-745cm, section 7 is from 745cm-965cm, and section 8 is from 965cm-1130cm. We did not account for years before 1905 since some cores did not go back that far.





**Figure 11: Pictures of CMF Coral slab sections 1, 2, 3, 4, 5, 6, 7, 8, and 9 before scanning by XRF.** Section 1 accounts for years 2005-1988, section 2 is from 1988-1967, section 3 accounts for 1966-1940, section 4 accounts for 1940-1934, section 5 accounts for 1934-1925, section 6 accounts for 1925-1915, section 7 accounts for 1925-1902. The other two final sections account for years 1902-1862, which we do not account for in this study. These three pictures are CMF coral slab sections 1 & 2 are in the top part of the figure, sections 3, 4, 5, & 6 are in the middle of the figure, and sections 7, 8, & 9 are at the bottom. Section one is 55cm-155cm and section two is from 155-300cm. Section 3 is from 100-315 cm, section 4 is from 315-380cm, section 5 is from 380 to 460cm, section 6 is from 460 to 560cm. Section 7 is from 30-140cm, section 8 is from 140-260cm, and section 9 is from 260-515cm. These photographs were taken with the XRF camera. These were scanned separately since the pieces did not fit well together. Jessica Carilli scanned all CMF sections.

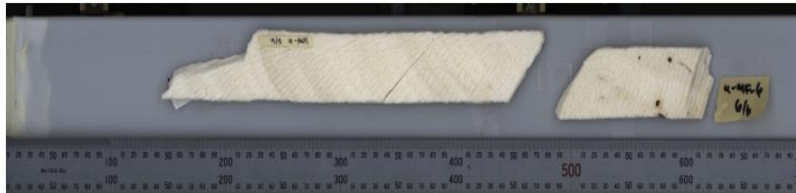
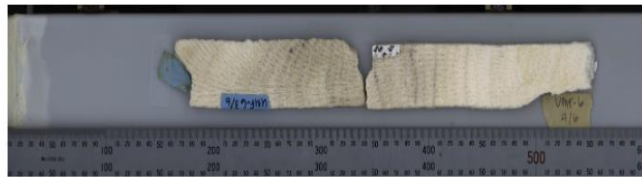


**Figure 12: Pictures of UMF Coral slab sections 1, 2, 3, 4, 5, 6, and 7 before scanning by XRF.** These three pictures are XRF pictures of UMF coral slab sections 1 & 2 which are featured on the top of the figure, sections 3 & 4 which are in the middle of the figure, and sections 5, 6, & 7 which are at the bottom of the figure. Section 1 & 2 account for years 2004-1978, section 3 accounts for 1979-1963, section 4 accounts for 1963-1935, section 5 accounts for part of 1936 and then from 1935-1911, and finally section 6 accounts for 1911-1905. Section 7 was not accounted for since the growth bands began to become vertical instead of horizontal which makes XRF unable to measure them accurately. Section 1 starts at 55cm and ends at 135cm. Section 2 starts at 135cm and ends at 290cm. Section 3 starts at 180cm and ends at 340cm. Section 4 starts at 340cm and ends at 550cm. Section 5 actually begins at 210cm since the XRF scans down the middle and ends at 360cm. Section 6 begins at 360 cm and ends at 460cm. Section 7 begins at 500cm and ends at 620cm. The same is true for UMF data as for CMF data in concerns to separate scans and time constraints.

## RESULTS



We correlated our X-Ray Fluorescence (XRF) data against the Inductively Coupled Plasma Mass Spectrometry (ICP-MS) data, which was conducted by Jessica Carilli and measures only purely substituted metals, to determine if XRF was measuring substituted metal or trapped metal. We then correlated XRF measurements for resistant phases (metals unlikely to be substituted within the coral lattice) to determine if XRF was measuring trapped metal. We did this by finding the annual average accumulation of metal within the coral lattice across all sites. The XRF determined counts of metal accumulation every two millimeters along the coral slabs. We then averaged these measurements according to the annual extension rates via an age model and determined the annual average metal accumulation within the coral lattice. We used ratios of the annual average metal accumulation against, Calcium, the most abundant element. Carilli did this with her data from the ICP-MS; to compare our data we needed to utilize ratios of the annual accumulation of the chosen elements (Ba, Cr, Cu, Mn, Pb, Sb, Zn) against annual Calcium measurements from the XRF data. We used a regression technique to determine if there was high correlation ( $>.7$ ) between XRF and ICP-MS data. We determined there was no high correlation between XRF and ICP-MS values.

- (a) **Age model:** XRF data from the coral slabs gave us measurements of metal content in correlation to millimeters. We created an age model to correlate each XRF measurement of metal content along the coral slab to the year in which the coral calcified and the metal accumulated in the coral skeleton. We utilized x-ray pictures taken of each coral (figure 8), which provided us with the length in millimeters that the coral grew annually. We used the coral growth rates, annual density banding, and the yearly extension rate of each coral slab (table 2) to determine this. Since, the XRF was calibrated to a 2mm resolution, (XRF took measurements every 2mm along the coral slab) we divided the total extension per year in millimeters by 2mm to determine the amount of XRF measurements per year along the coral slabs. This final model showed used which year the metal had accumulated and how much metal had accumulated.
- (b) **Comparison with ICP-MS data:** Carilli et al. 2009 chose seven metals: Ba, Cr, Cu, Mn, Pb, Sb, Zn. They were chosen because they tend to be indicators of environmental change and environmental history of the water, nearby land erosions rates, and human impacts.

These metals are indicators of a “variety of land-based sources ranging from terrigenous sedimentation to mining waste” (Prouty et al. 2008, Carilli et al., 2009). Carilli et al. (2009) utilized ratios of Ba/Ca, Mn/Ca, Cr/Ca, Sb/Ca, Cu/Ca, Pb/Ca, and Zn/Ca. Specifically, Barium/Calcium ratios are used as tracers for sediment runoff because Barium desorbs from terrigenous particles when fresh and saltwater mix (Alibert et al., 2003; McCulloch et al., 2003; Fleitmann et al., 2007; Carilli et al., 2009). Manganese/Calcium ratios track primary productivity, influenced by nutrients from rivers, therefore helping us to understand variations in terrestrial runoff (Abram et al. 2003, Alibert et al., 2003; Carilli et al., 2009). The other four metal ratios Zn/Ca, Pb/Ca, Mn/Ca, and Cu/Ca ratios were used to investigate runoff from mines close to coral reefs (Fallon et al., 2002; David 2003). For the purposes of comparison, we selected the ratios of Ba, Cr, Cu, Mn, Pb, and Zn to Calcium; all these metals were estimated by both the XRF and the ICP-MS methods.

Figures 13-16 depict the correlation between the XRF estimates and ICP-MS estimates for the six elements – (expressed as ratios) Barium (Ba), Lead (Pb), Chromium (Cr), Manganese (Mn), Copper (Cu), and Zinc (Zn). The value “n” on each of the graphs in figures 13-16 depicts the number of data points compared between ICP-MS and XRF. The  $R^2$  values in figures 13-16 show the level of correlation for XRF and ICP-MS data. In this study, we determine low correlation as anything below an  $R^2$  value of .2. ICP-MS and XRF values have low correlation for all six elements across all four sites.

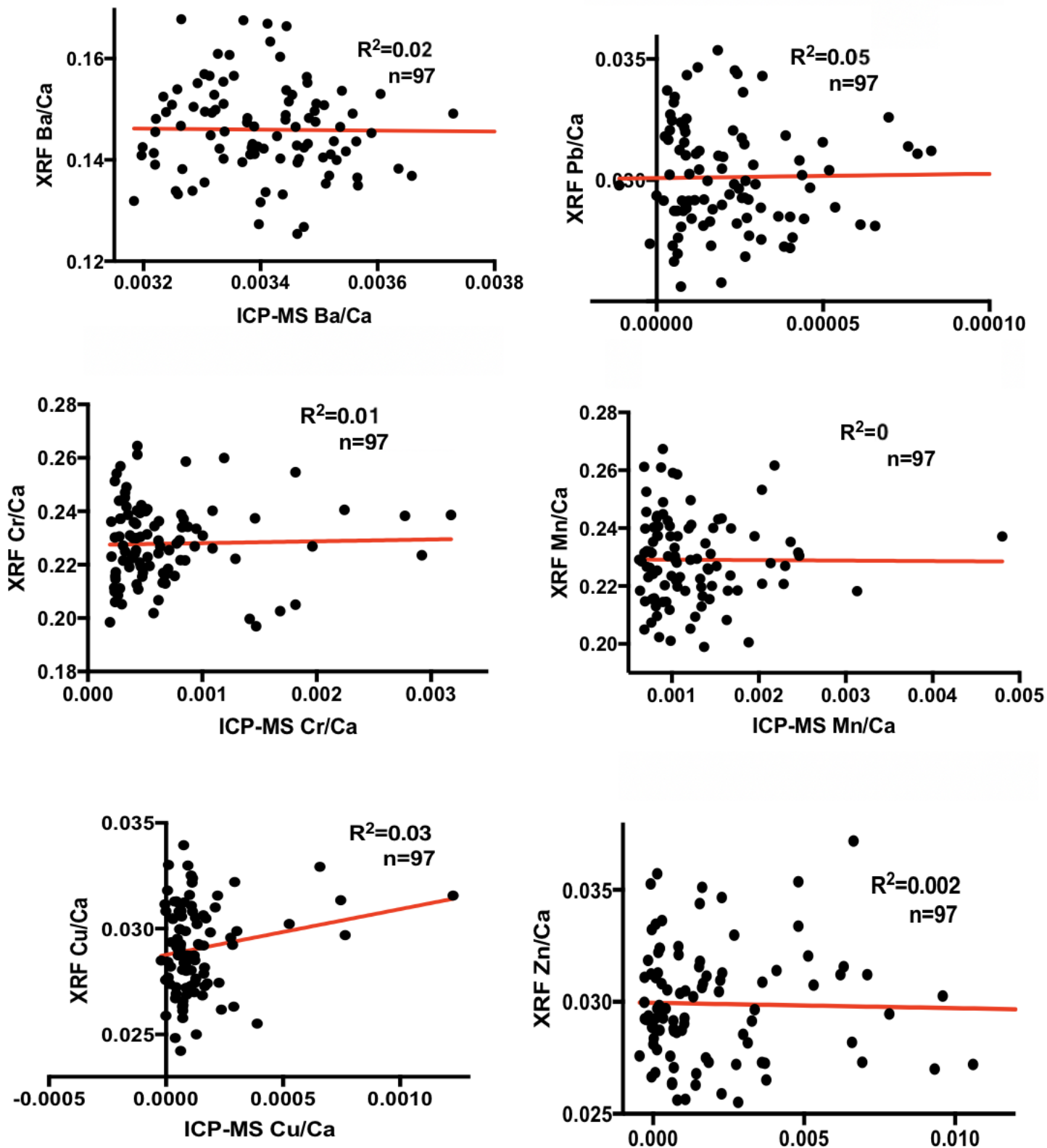


**Figure 13: Correlation of HMF ICP-MS data to XRF Data.** XRF data is on the Y axis and ICP-MS data is on the X axis. There were 97 points taken by the XRF and ICP-MS that were taken in the same spot on the coral slab and in the same years. The Ba series has an  $R^2$  of .018, the Pb has an  $R^2$  of .005, the Cr series has an  $R^2$  of .001, the Mn series has an  $R^2$  of almost zero, the Cu series has an  $R^2$  of .034, and the Zn series has an  $R^2$  of .002. Average correlation in this HMF series was .01.

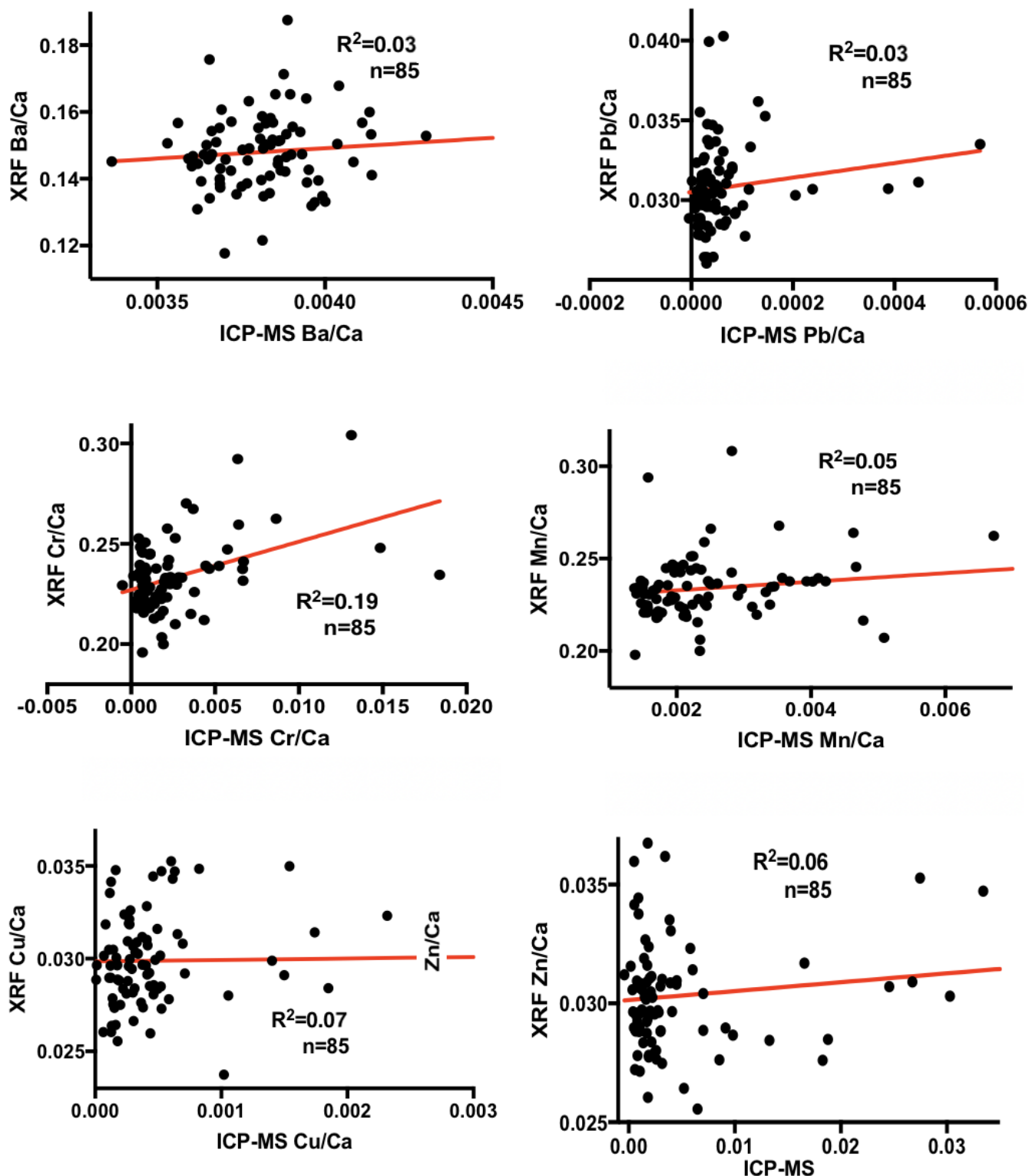
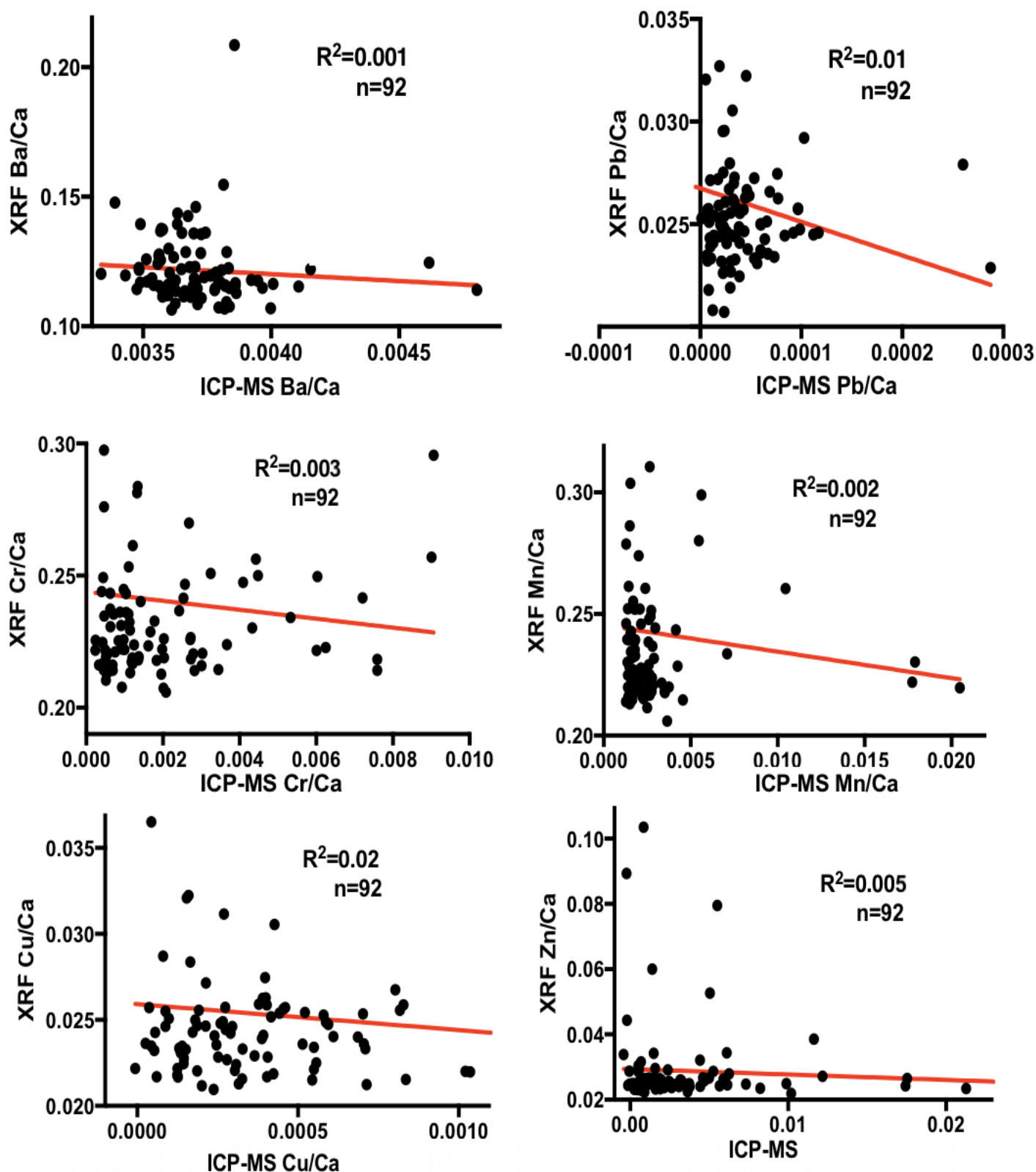
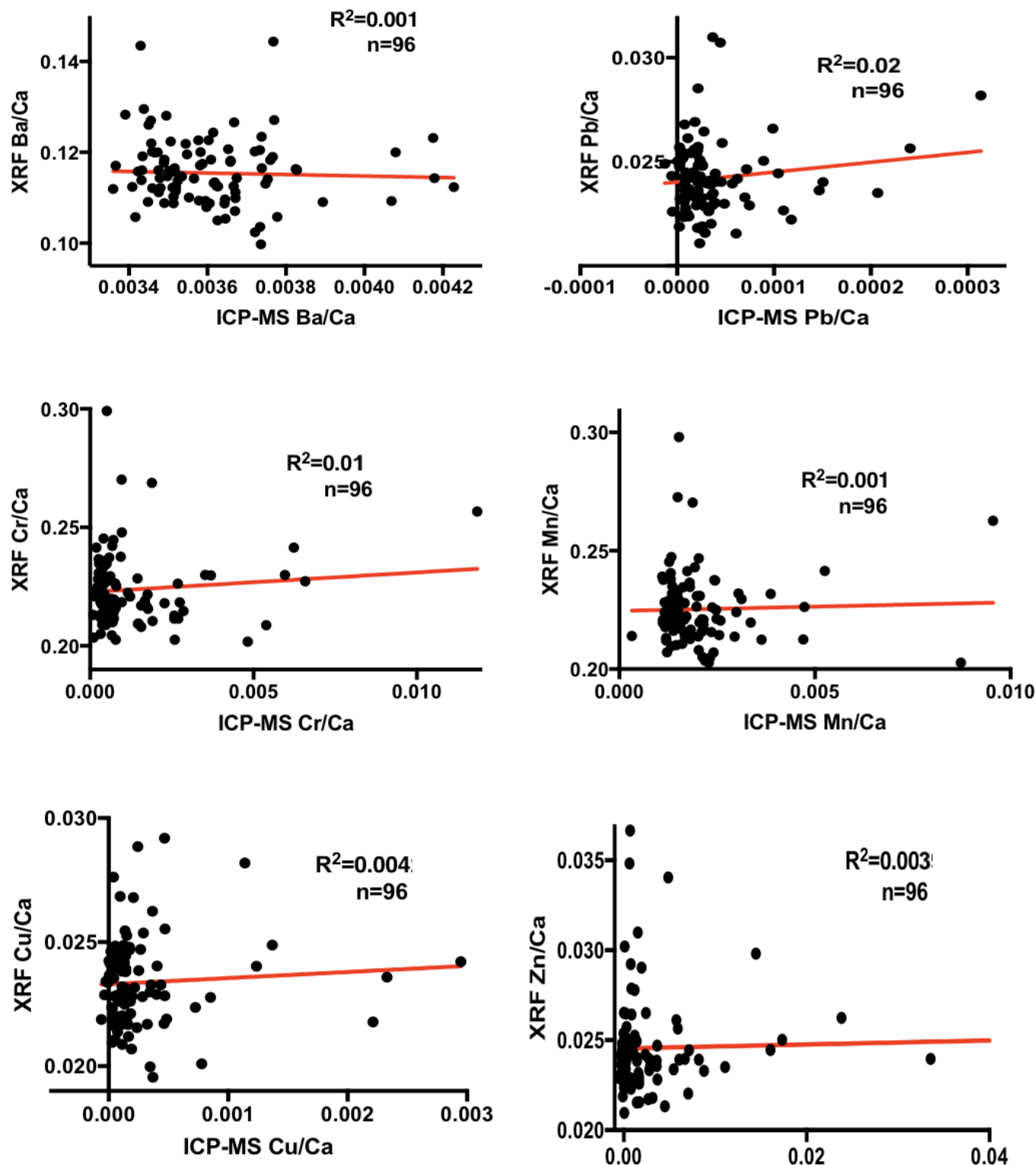


**Figure 14: Correlation of SMF ICP-MS data to XRF Data.** XRF data is on the Y axis and ICP-MS data is on the X axis. There were 85 points taken by the XRF and ICP-MS that were taken in the same spot on the coral slab and in the same years. The Ba series has an  $R^2$  of .025, the Pb has an  $R^2$  of .025, the Cr series has an  $R^2$  of .187, the Mn series has an  $R^2$  of .046, the Cu series has an  $R^2$  of .062, and the Zn series has an  $R^2$  of .061. However, due to a lower  $n$  value in SMF confidence in these numbers is lower. Average correlation in this SMF series was .068.



**Figures 15: Correlation of CMF ICP-MS data to XRF Data.** XRF data is on the Y axis and ICP-MS data is on the X axis. There were 92 points taken by the XRF and ICP-MS that were taken in the same spot on the coral slab and in the same years. The Ba series has an  $R^2$  of .007, the Pb has an  $R^2$  of .012, the Cr series has an  $R^2$  of .003, the Mn series has an  $R^2$  of .003, the Cu series has an  $R^2$  of .015, and the Zn series has an  $R^2$  of .005. We have a higher confidence in CMF due to the n value being 92. Average correlation in this SMF series was .008.



**Figures 16: Correlation of UMF ICP-MS data to XRF Data.** XRF data is on the Y axis and ICP-MS data is on the X axis. There were 96 points taken by the XRF and ICP-MS that were taken in the same spot on the coral slab and in the same years. The Ba series has an  $R^2$  of .001, the Pb has an  $R^2$  of .019, the Cr series has an  $R^2$  of .009, the Mn series has an  $R^2$  of .001, the Cu series has an  $R^2$  of .004, and the Zn series has an  $R^2$  of .003. We have a higher confidence in UMF due to the  $n$  value being 96. Average correlation in this SMF series was .006.

Our observations of the correlations between XRF and ICP-MS data are as follows:

- No significant correlation ( $R^2 > .7$ ) between XRF data and ICP-MS data for all six metals
- No medium correlation ( $.4 < R^2 < .6$ ) between XRF data and ICP-MS data for all six metals
- Only low correlation ( $R^2 < .4$ ) between XRF data and ICP-MS data for all six metals

Note that Carilli et al. 2009 identified another metal element that tracks soil erosion: Antimony (Sb). However, XRF does not measure Sb, so we were unable to correlate our data with that metal. Essentially, there was no significant correlation between XRF measurements and ICP-MS measurements for the Belize coral cores at all four sites. If there had been we could conclude with some confidence that XRF was measuring substituted metal within the coral skeleton. Since we determined that XRF was not measuring substituted metal, we wanted to show that XRF was measuring trapped metal in the coral skeleton. We did this by correlating XRF values of resistant metals (metals most likely to become trapped).

**(c) Characterizing resistant phases:** Next we correlated XRF data for resistant metals (metals not likely to substitute within the coral lattice). If these metals accumulated in the coral skeleton at a similar rate it may reveal that these metals accumulated in the waters surrounding these corals from a variety of processes relating to soil erosion, mining, etc. High correlation values ( $> .7$ ) between two resistant metals gave us confidence that these resistant metals were being incorporated within the coral lattice at the same rate, thereby showing that a single process (soil erosion, mining, etc.) may be the reason for their accumulation in the coral lattice. Medium correlation ( $.4 < R^2 < .6$ ) and low correlation ( $R^2 < .4$ ) gave us less confidence that the metals were accumulating at the same rate within the coral lattice. By showing that the XRF data for resistant metals correlated, we showed that XRF measures purely trapped metal.

We chose commonly occurring metals in the waters near the Belizean coast. Note that each of these metals are carried either in solution or as a discrete mineral particle. But, because our method does not track chemical substitution, we believe that the metals exist within discrete minerals (oxides or silicates); for example, zirconium is delivered by zircon ( $\text{ZrSiO}_4$ ) and titanium (Ti) is delivered by rutile ( $\text{TiO}_2$ ). Since Zr and Ti have large cations, these metals

cannot be substituted chemically and can only exist as resistant discrete mineral grains trapped within cavities. We use these to assess the behavior of other metals commonly found in the coastal water of Belize, for example, Barium and Strontium represent sediment erosion, Manganese and Zinc represent mine waste, and Titanium and Zircon represent processes relating to dust and soil (Carilli et al. 2010). We suggest that a high correlation between the cations with Zr and Ti will reveal that these are hosted in mineral grains that are released from a variety of processes relate to soil erosion, mining etc. We looked at the following cations since they were hosted within resistant mineral phases. Titanium and Zircon were chosen specifically because they are resistant to dissolution and have the highest likelihood of being trapped, instead of substitution within the coral lattice. Titanium and Zircon cations cannot be substituted because of their large size. The resistant cations were chosen because they commonly occur in mineral phases derived from soil erosion and are not easily digested by acids or bases. Zircon and Titanium often are purely trapped so having them on the x-axis helps to compare to other supposedly trapped metals Aluminum and Iron. These metals can sometimes be substituted but can also become purely trapped metal. (Barnard et al. 1974).

Figures 17-20 are correlations XRF data for metals at all four sites. We determined general correlations for each series as low correlation ( $<.4$ ), medium correlation ( $.4 < R^2 < .6$ ), or high correlation ( $>.7$ ). We made correlations for resistant metals (Ti, Zr, Al, and Fe) and other metals Sr, Ba, Mn and Zn. Each figure shows the number of correlated values (n) and the correlation values ( $R^2$ ). Table 6 gives a summary of correlation values for resistant metals from figures 17-20.



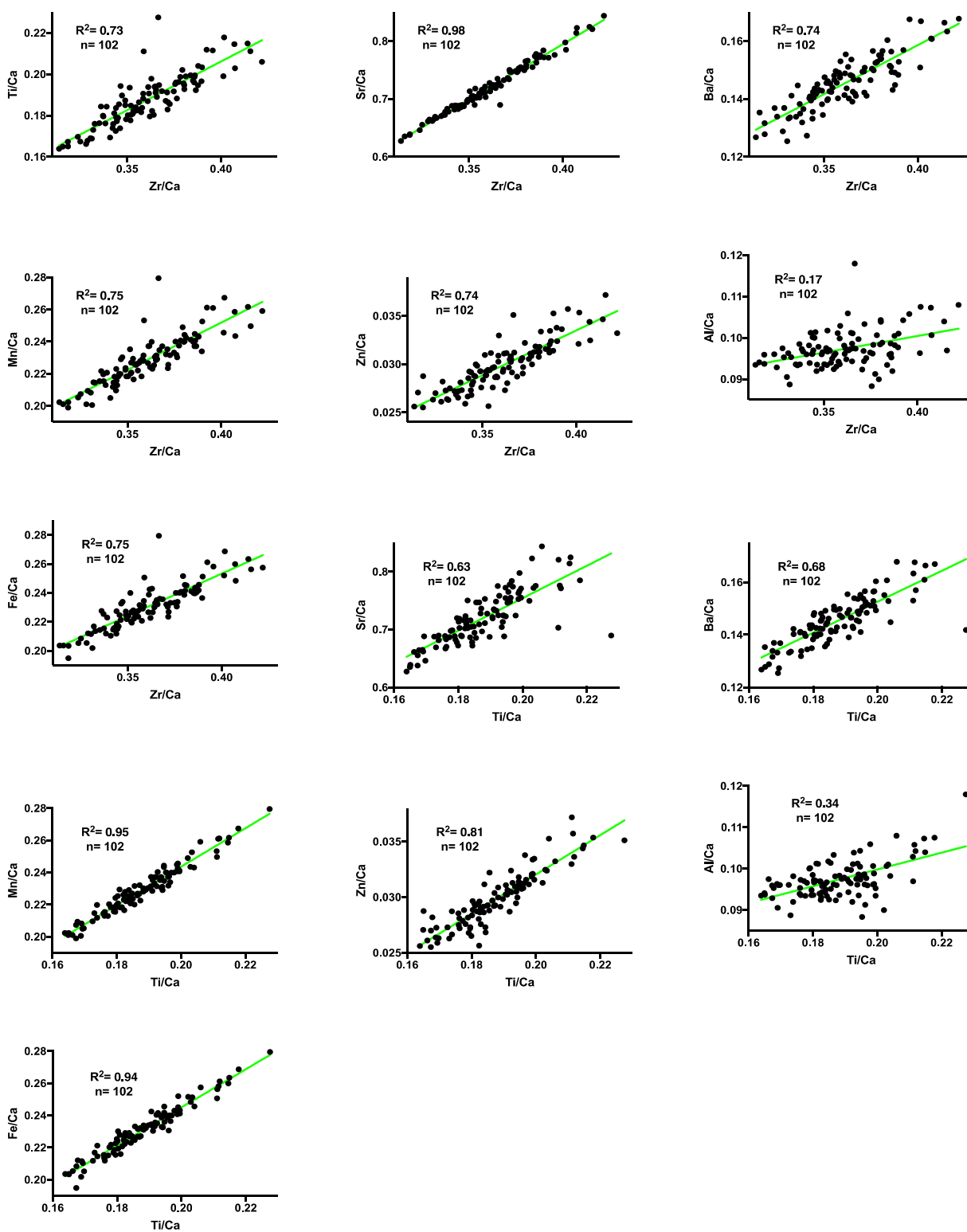


**Figure 17: Correlation of resistant metals (Ti, Zr, Al, and Fe) and other metals Sr, Ba, Mn and Zn from XRF at HMF site. HMF site, which is north of Belize, has the least “continental influence” (Carilli 2009) meaning less sediment runoff.**

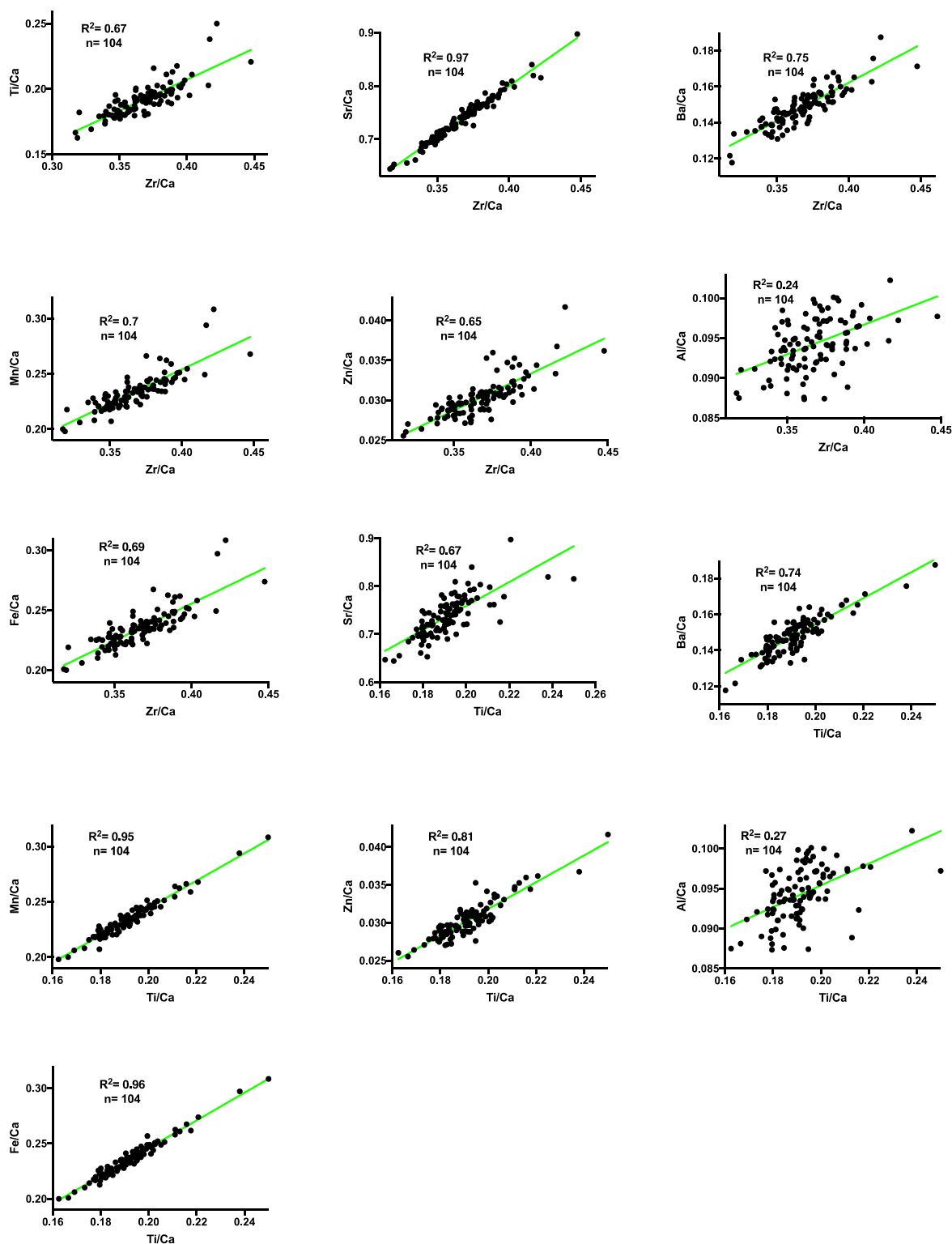


**Figure 18: Correlation of resistant metals (Ti, Zr, Al, and Fe) and other metals Sr, Ba, Mn and Zn from XRF at SMF site.** The SMF site which is in the Gulf of Honduras and may experience runoff due to high mountain ranges as well as a “counter clockwise gyre that spins off the main northwesterly flowing Caribbean current” (Carilli 2009, Burk and Sagg 2006, Thattai et al. 2003).

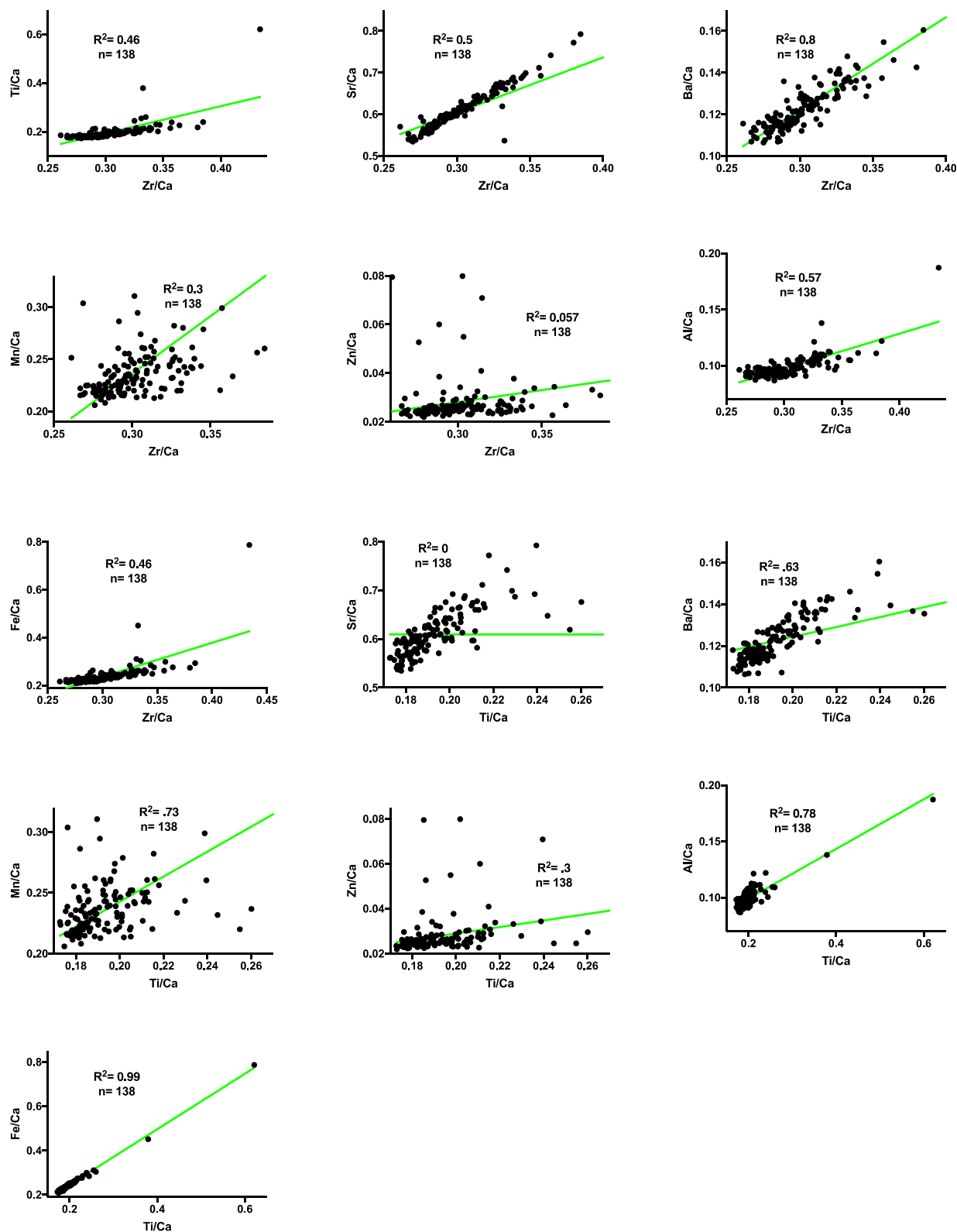


**Figure 19: Correlation of resistant metals (Ti, Zr, Al, and Fe) and other metals Sr, Ba, Mn and Zn from XRF at CMF site. The CMF site had the second most “continental influence (Carilli 2009).**

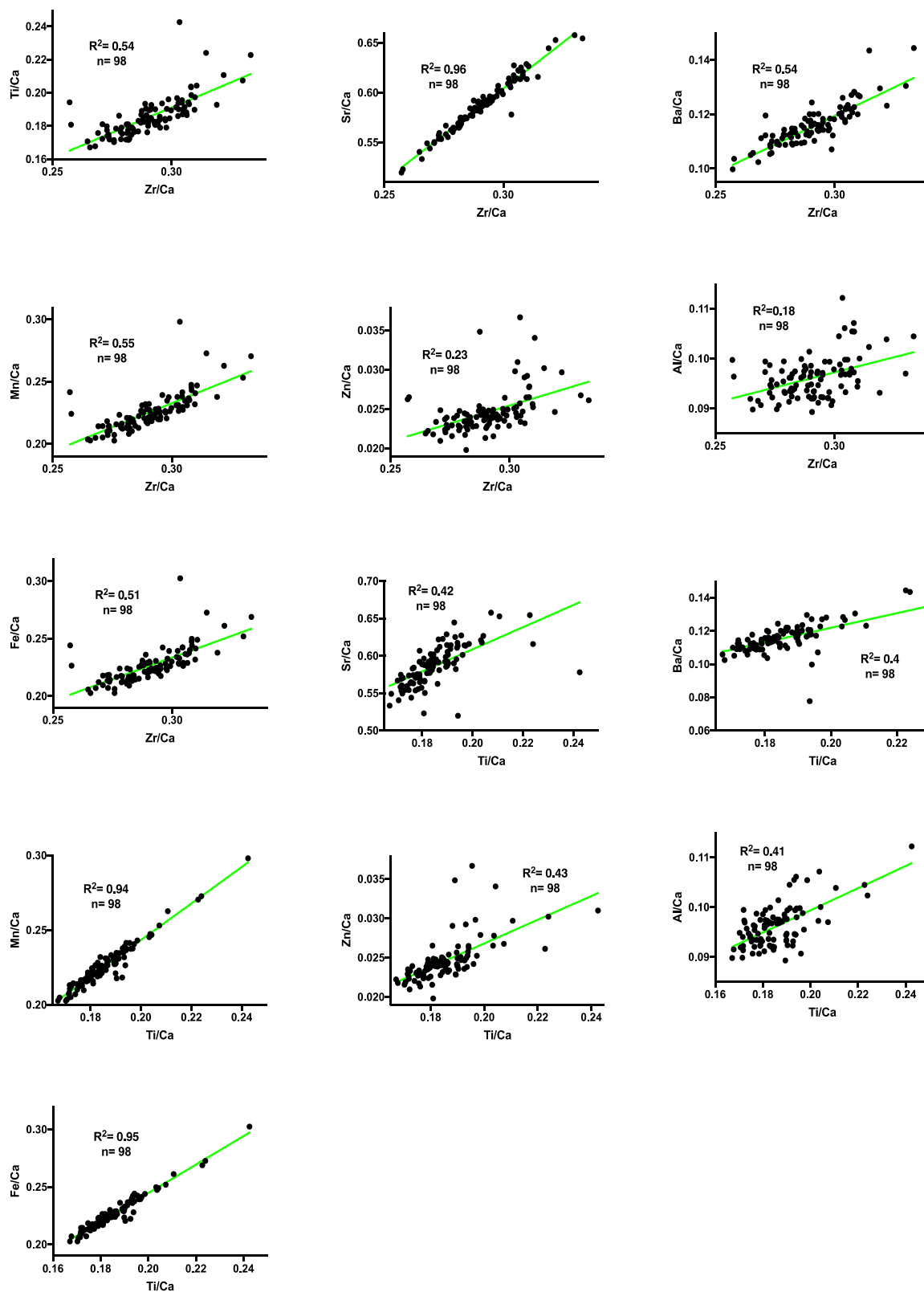


**Figure 20: Correlation of resistant metals (Ti, Zr, Al, and Fe) and other metals Sr, Ba, Mn and Zn from XRF at UMF site. Utila had the “third most continental influence” (Carilli 2009).**

Our key observations from figures 17-20 and listed in table (6) are as follows

HMF correlation values from 102 data points

- Ti:Zr (.7), Fe:Zr (.8), and Fe:Ti (.9) have high correlation
- Al:Zr (.2) and Al:Ti (.3) have low correlation

SMF correlation values from 104 data points

- Fe:Ti (.9) have high correlation
- Ti:Zr (.7) and Fe:Zr (.7) have medium correlation
- Al:Zr (.2) and Al:Ti (.3) have low correlation

CMF correlation values from 138 data points

- Fe:Ti (1) and Al:Ti (.8) have high correlation
- Al:Zr (.6), Ti:Zr (.5), and Fe:Zr (.5) have medium correlation

UMF correlation values from 98 data points

- Fe:Ti (1) have high correlation
- Ti:Zr (.5), Fe:Zr (.5), and Al:Ti (.4) have medium correlation
- Al:Zr (.2) has low correlation

By correlating XRF measurements of resistant cations (Ti, Zr, Al, and Fe) we determined that many of these cations have high correlations ( $>.7$ ) (there are 7 instances of high correlations across all four sites out of the 20 correlations) and we can effectively show that XRF is measuring trapped metal within the coral lattice. Medium correlations ( $.6 < R^2 < .4$ ) help to further prove that XRF is measuring trapped metal (another 8 instances of medium correlations for a total of 15/20 correlations resulting in high to medium correlation values).

Aluminum, however, had lower correlations to other resistant metals. Some additional sources or processes could be playing into how aluminum was incorporated into the coral skeleton. Aluminum could potentially be influenced by anthropocentric cement activities (Carilli 2009) from the coast and therefore not be accumulating at the same rate as other resistant metals.

**Table 6: Correlation  $R^2$  value for metals from all four sites:** Metals with  $R^2$  values of over .7 were considered to be highly correlated, .4-.7 is medium correlated, and anything below .4 was considered to not be correlated. The metals below are ratios of Al, Zr, Ti, and Fe against calcium taken by measurements with the XRF machine.

<b><math>R^2</math> Value</b>	<b>Al/Ca vs. Zr/Ca</b>	<b>Ti/Ca vs. Zr/Ca</b>	<b>Fe/Ca vs. Zr/Ca</b>	<b>Fe/Ca vs. Ti/Ca</b>	<b>Al/Ca vs. Ti/Ca</b>
<b>HMF</b>	.17	.73	.75	.94	.34
<b>SMF</b>	.24	.67	.69	.96	.27
<b>CMF</b>	.57	.45	.46	.99	.78
<b>UMF</b>	.18	.54	.51	.95	.41
<b>Average</b>	.29	.60	.60	.96	.45

## DISCUSSIONS AND CONCLUSIONS

Due to the low correlation between X-Ray Fluorescence (XRF) and Inductively Coupled Plasma Mass Spectrometer (ICP-MS), we believe that XRF does **not** measure substituted metal. Due to the existence of high correlations ( $>.7$ ) and medium correlations ( $.6 > R^2 > .4$ ) between XRF measurements of resistant cations, we determined that XRF is measuring trapped metal. We did not find any significant correlation ( $>.7$ ) nor did we find any instance of medium correlation ( $0.6 > R^2 > 0.4$ ) between ICP-MS and XRF data. The average correlation value for XRF vs. ICP-MS data across all four sites for 370 points was .02475. Based on these results, we conclude that XRF does not measure substituted metals.

Figures 17-20 of XRF measurements show that there are strong covariations between the pairs:

HMF - Zr:Ti, Zr:Sr, Zr:Ba, Zr:Mn, Zr:Zn, Zr:Fe, Ti:Mn, Ti:Zn, and Ti:Fe

SMF - Zr:Sr, Zr:Ba, Zr:Mn, Ti:Ba, Ti:Mn, Ti:Zn, and Ti:Fe

CMF: Zr:Ba, Ti:Mn, Ti:Al, Ti:Fe

UMF: Zr:Sr, Ti:Mn, Ti:Fe

The narrative put forth by Carilli that the sites in this study have decreasing degrees of influence from land based activities (SMF being the most heavily polluted, CMF second, UMF third, and finally HMF) does not hold when simply looking at the number of XRF measurements of strong covariations for resistant metals. HMF experienced the least amount of sedimentation (Carilli 2009) but still shows numerous high covariation values between metals measured by XRF. SMF experiences the highest levels of sedimentation, according to relative Ba/Ca ratios (Carilli 2009); this actually does correspond to the high number of strong covariation values from the XRF. The SMF site has been experiencing declining growth rates since the 1970s which is attributed to high sedimentation rates (Carilli 2009); so the presence of multiple strong covariations between resistant metals (which may be deterministic of land based processes such as agriculture and mining) may be a factor for these slow growth rates. Both HMF and SMF sites are in proximity to land that has seen increasing land use and development (Carilli 2009). High covariance of metals at each site is not unexpected and may be a result of the "random and erratic" (Goreau 1977) way in which the skeletal material uptakes these metals, which could explain why HMF had more instances of strong covariation between resistant metals than SMF.

Overall, we see a decadal pattern of variation in all the pairs, which we take to reflect a variation in amounts of trapped material. This is not due to changes in source, since Ti:Zr represents resistant phases, Sr:Ba represents soil erosion, and Zn:Mn indicates mining activities. This could reflect a role of large scale climate (rainfall tied to regional and global) which often exhibits a decadal pattern and therefore reflects control of runoff of all materials.

We do not see any trend in the XRF data (figures 21-24). This indicates that the accumulation of trapped material may be reflective of the rate of formation of cavities: more accumulation of trapped material during times of stress and less during times of little and no stress. This could be controlled by the temperature of the water regulated by the ocean and climate dynamics. El Niño could be important as the 1998 El Niño seems to align with high accumulations of metal measured by the XRF across all sites. We also see muted degree of variations as we move away from CMF (the most polluted site) and that could be a function of fewer particles in the ocean water.

High correlations among resistant cations show potential promise for further understanding the effects of outside sources on metal accumulation within corals. For example, Iron and Titanium correlated extremely well in all four sites (table 6). Reasons for strong correlations between these metals could be the fact that there is heavy runoff from agricultural and industrial activities. These metals are commonly found within soil coming from runoff (Carilli et al., 2009) and their high correlation across all four sites points towards them coming from the same source.

Figures 21-24 show the annual accumulation of eight metals measured by XRF: Zircon, Titanium, Iron, Strontium, Barium, Manganese, Zinc and Aluminum. Strontium and Barium are put on a single graph because they represent sediment erosion. Manganese and Zinc are put on a single graph because they represent mine waste. Titanium and Zircon are put on a single graph because they are the resistant cations, and are therefore all trapped metals. Aluminum and Iron are on a single graph because they can be both substituted and trapped. The graphs in the series do not show any trend. However, the existence of generally high correlation values between the cations with Zr and Ti and the other metals (Fe, Sr, Ba, Mn, Zn, and Al) reveals that they are



hosted in mineral grains that are released from a variety of processes relate to soil erosion, mining etc.

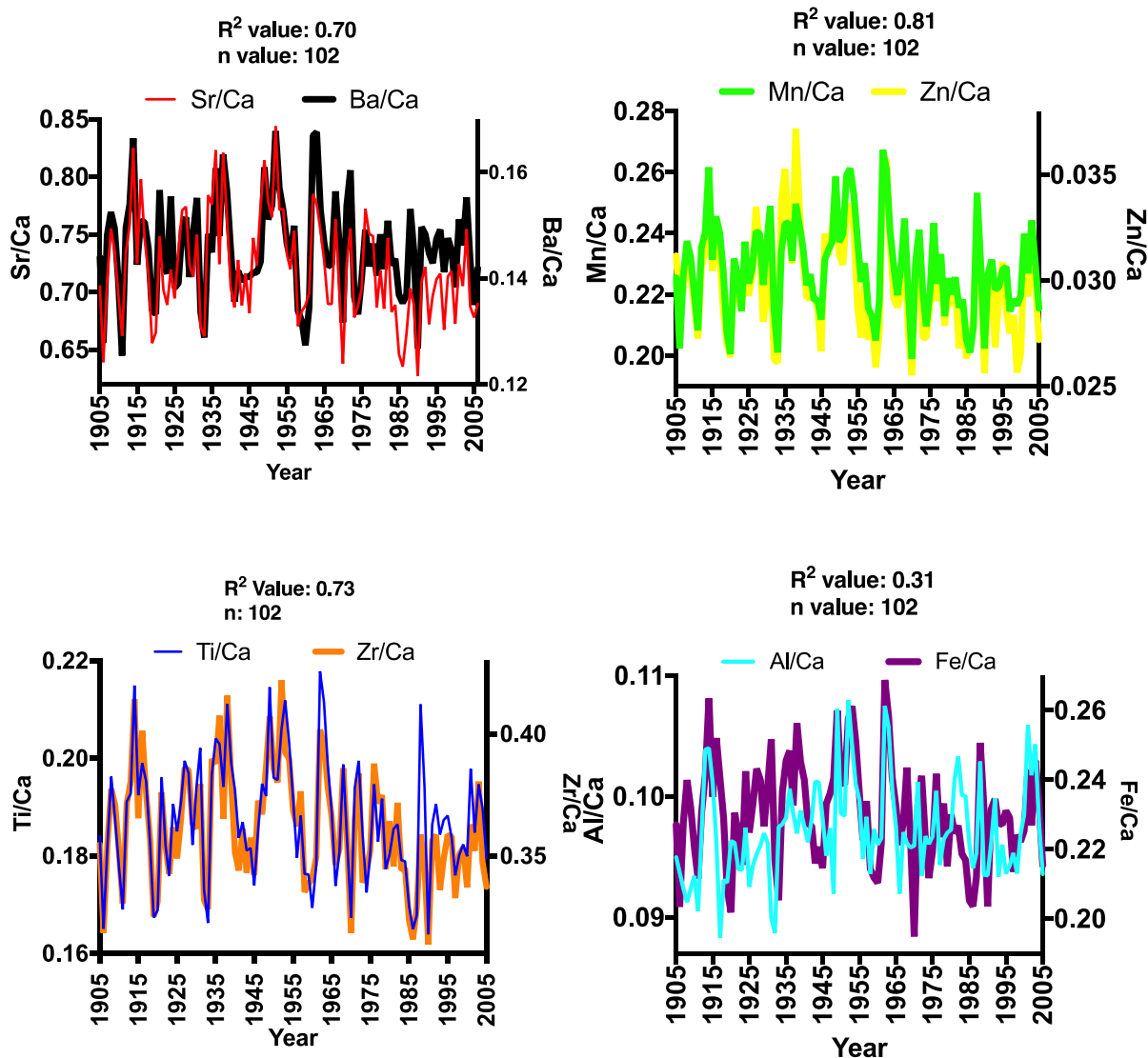


**Figure 21: Time Series for metals Sr, Ba, Mn, Zn, Ti, Zr, Al, and Fe at HMF Site taken with XRF data.** All HMF time series start in the year 1905. Strontium and Barium are put on a single graph because they represent sediment erosion. Manganese and Zinc are put on a single graph because they represent mine waste. Titanium and Zircon are put on a single graph because they are the resistant cations, and are therefore all trapped metals. Aluminum and Iron are on a single graph because they can be both substituted and trapped making them unique among the elements measured.

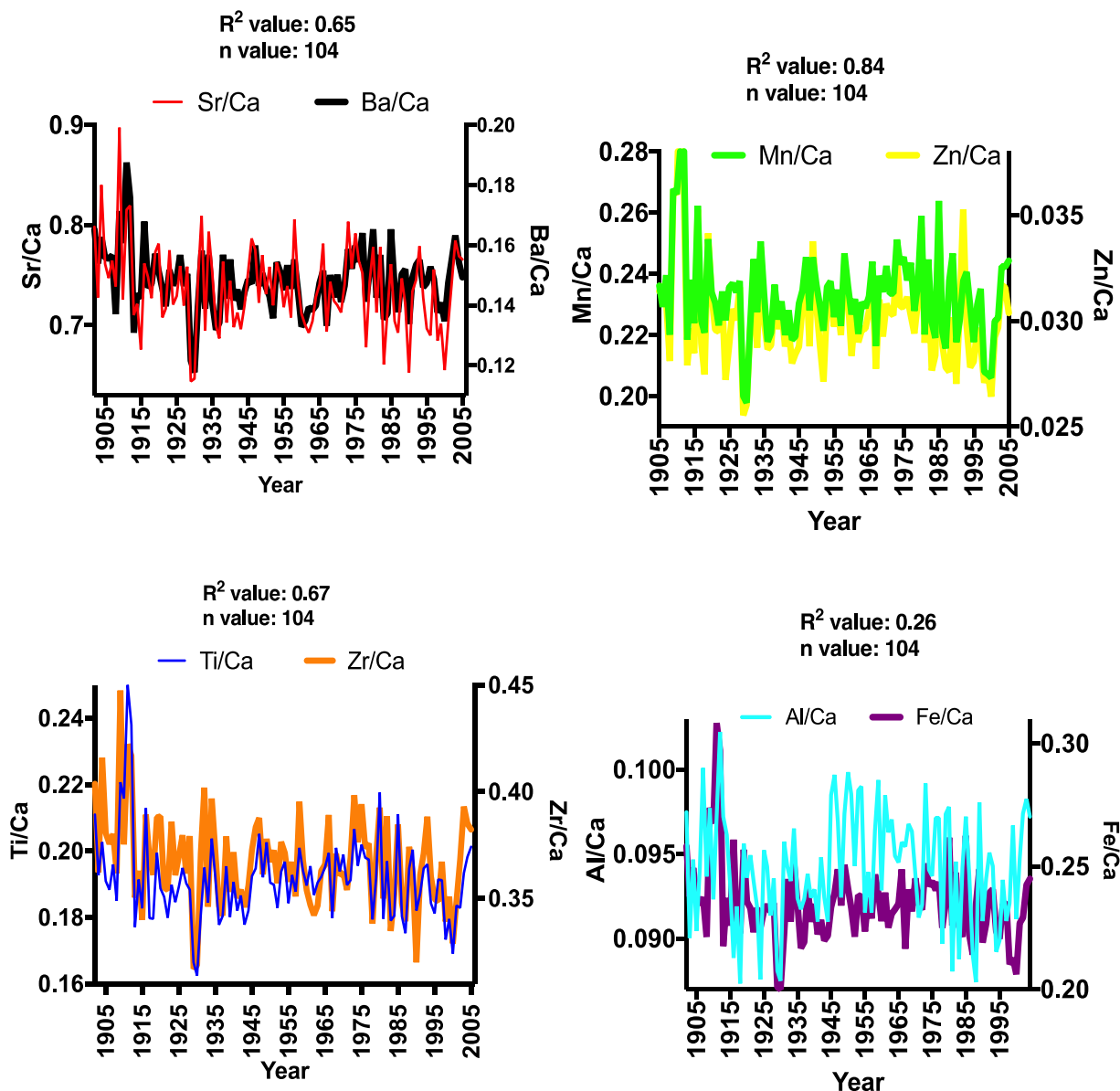


**Figure 22: Time Series for metals Sr, Ba, Mn, Zn, Ti, Zr, Al, and Fe at SMF Site taken with XRF data.** All SMF time series start in the year 1905. Strontium and Barium are put on a single graph because they represent sediment erosion. Manganese and Zinc are put on a single graph because they represent mine waste. Titanium and Zircon are put on a single graph because they are the resistant cations, and are therefore all trapped metals. Aluminum and Iron are on a single graph because they can be both substituted and trapped making them unique among the elements measured.

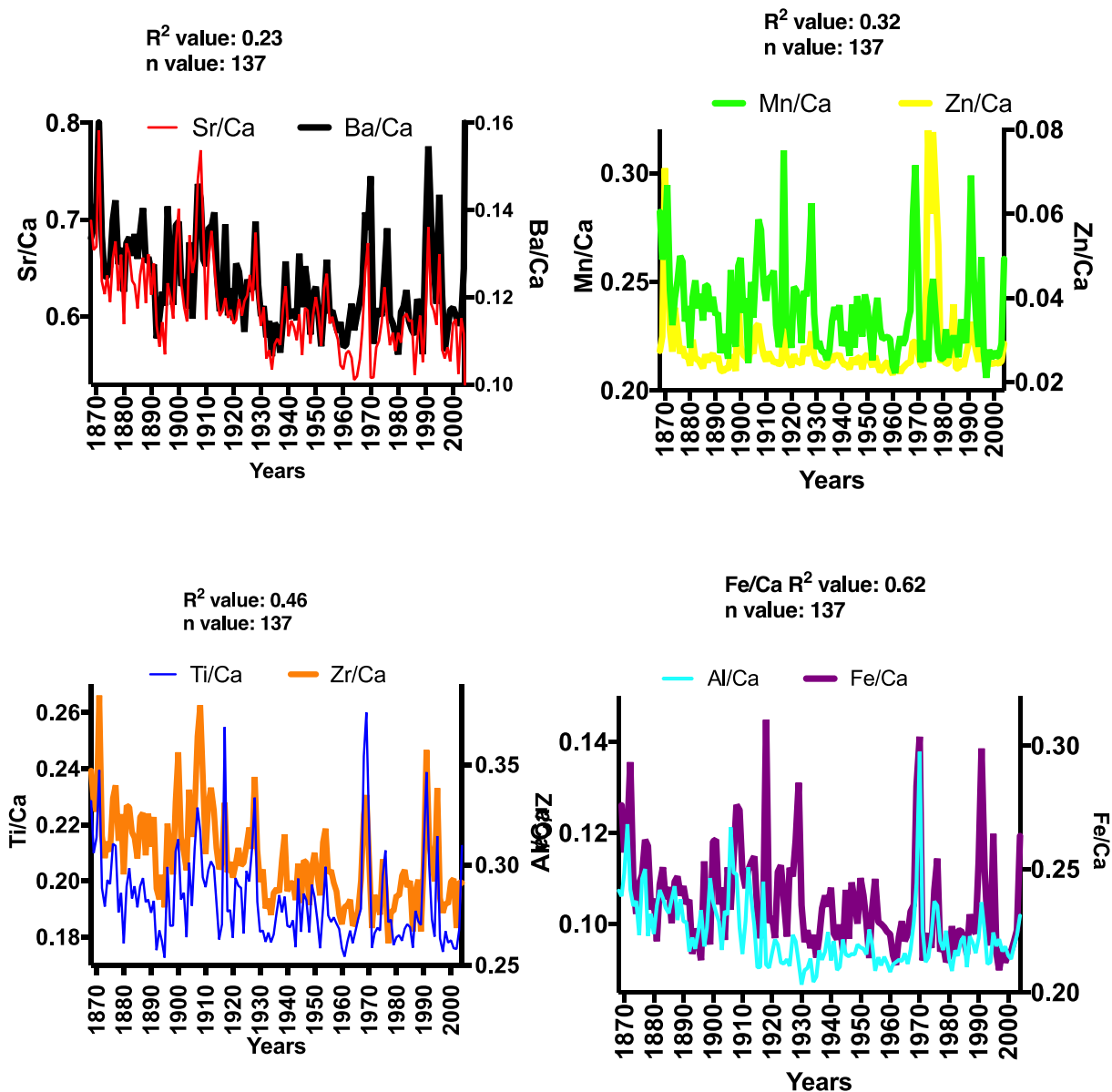


**Figure 23: Time Series for metals Sr, Ba, Mn, Zn, Ti, Zr, Al, and Fe at CMF Site taken with XRF data.** All CMF time series start in the year 1876. Strontium and Barium are put on a single graph because they represent sediment erosion. Manganese and Zinc are put on a single graph because they represent mine waste. Titanium and Zircon are put on a single graph because they are the resistant cations, and are therefore all trapped metals. Aluminum and Iron are on a single graph because they can be both substituted and trapped making them unique among the elements measured.

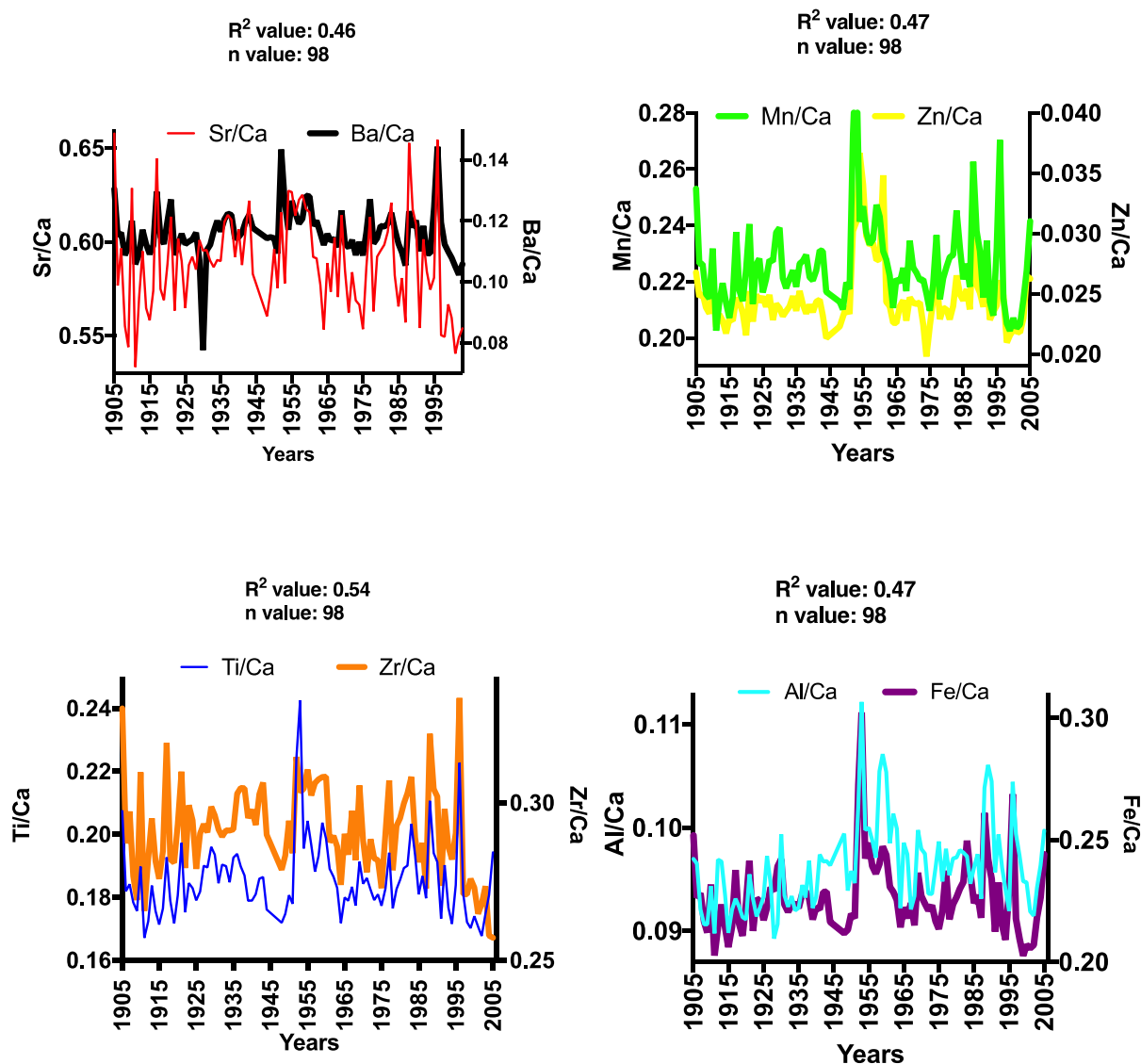


**Figure 24: Time Series for metals Sr, Ba, Mn, Zn, Ti, Zr, Al, and Fe at UMF Site taken with XRF data.** All UMF time series start in the year 1905. Strontium and Barium are put on a single graph because they represent sediment erosion. Manganese and Zinc are put on a single graph because they represent mine waste. Titanium and Zircon are put on a single graph because they are the resistant cations, and are therefore all trapped metals. Aluminum and Iron are on a single graph because they can be both substituted and trapped making them unique among the elements measured.

## **RECOMMENDATION FOR FUTURE WORK IN CORAL STUDIES**

X-Ray Fluorescence (XRF) is a viable tool for understanding the accumulation of trapped metal within the coral lattice. As Barnard et al. (1974) stated, “the inclusion of trapped material in understanding the effects of metal particulate matter on the health of corals is instrumental to understanding the full picture”. XRF offers a quick, non-destructive, and cheap method for understanding trapped metal. In the future, coral proxy tools used for understanding the accumulation of metals throughout the years can be more precise and more inclusive by utilizing trapped metal accumulation data. With XRF, scientists can obtain a more accurate understanding of the environmental and climactic history of the water in which corals grew.

Furthermore, few studies have determined the effects of particulate matter on the health of corals. With a better understanding of trapped metal, in addition to substituted metal, coral researchers can determine whether or not these metals are harming the structural stability of the coral, the health of the polyps, and the health of the surrounding ecosystem.

In order to further prove that XRF is a viable tool for coral studies, future studies should compare ICP-MS data to XRF data for different coral samples from different locations. With a more developed analysis of the correlation between ICP-MS values and XRF values in different coral samples we can further provide evidence that XRF measures purely trapped metal.

## Bibliography

- Abram, N. J. "Coral Reef Death During the 1997 Indian Ocean Dipole Linked to Indonesian Wildfires." *Science*, vol. 301, no. 5635, 2003, pp. 952–955., doi:10.1126/science.1083841.
- Alibert, Chantal, et al. "Source of Trace Element Variability in Great Barrier Reef Corals Affected by the Burdekin Flood Plumes." *Geochimica Et Cosmochimica Acta*, vol. 67, no. 2, 2003, pp. 231–246., doi:10.1016/s0016-7037(02)01055-4.
- Barnard, L. A., et al. "Possible Environmental Index in Tropical Reef Corals." *Nature*, vol. 252, no. 5480, 1974, pp. 219–220., doi:10.1038/252219a0.
- Bak, R. P. M. , and J. H. B. W. Elgershuizen. "Patterns of oil-Sediment rejection in corals." *Deep Sea Research*, vol. 24, no. 4, 1976, pp. 182–183., doi:10.1016/0146-6291(77)90012-1.
- Barnes, Harold, et al. *Oceanography and Marine Biology, An Annual Review*. 2003.
- Bastidas, C., et al. "Sedimentation rates and metal content of sediments in a Venezuelan coral reef." *Marine Pollution Bulletin*, vol. 38, no. 1, 1999, pp. 16–24., doi:10.1016/s0025-326x(99)80007-1.
- Berry, Kathryn L. E., et al. "Sources and spatial distribution of heavy metals in scleractinian coral tissues and sediments from the Bocas del Toro Archipelago, Panama." *Environmental Monitoring and Assessment*, vol. 185, no. 11, 2013, pp. 9089–9099., doi:10.1007/s10661-013-3238-8.
- Burke, Laurette, and Zachary Sugg. "Hydrologic Modeling of Watersheds Discharging Adjacent to the Mesoamerican Reef ." Research Gate, World Resources Institute, 1 Dec. 2006, [www.researchgate.net/profile/Zachary\\_Sugg/publication/279678164\\_Hydrologic\\_Modeling\\_of\\_Watersheds\\_Discharging\\_Adjacent\\_to\\_the\\_Mesoamerican\\_Reef\\_Analysis\\_Summary\\_-\\_December\\_1\\_2006/links/55c4ccd108aebc967df37ff1.pdf](http://www.researchgate.net/profile/Zachary_Sugg/publication/279678164_Hydrologic_Modeling_of_Watersheds_Discharging_Adjacent_to_the_Mesoamerican_Reef_Analysis_Summary_-_December_1_2006/links/55c4ccd108aebc967df37ff1.pdf). Web.
- Carilli, Jessica E., et al. "Century-Scale Records of Land-Based Activities Recorded in Mesoamerican Coral Cores." *Marine Pollution Bulletin*, vol. 58, no. 12, 2009, pp. 1835–1842., doi:10.1016/j.marpolbul.2009.07.024.
- Chen, Xuefei, et al. "Decadal variations in trace metal concentrations on a coral reef: Evidence from a 159 year record of Mn, Cu, and V in a Porites coral from the northern South China Sea." *Journal of Geophysical Research: Oceans*, vol. 120, no. 1, 2015, pp. 405–416., doi:10.1002/2014jc010390.
- Croudace, I. W., and R. G. Rothwell. *Micro-XRF studies of sediment cores: applications of a non-Destructive tool for the environmental sciences*. Dordrecht, Springer, 2015.

- Crustal Geophysics and Geochemistry Science Center. “Laser Ablation ICP-MS Laboratory.” *USGS Crustal Geophysics and Geochemistry Science Center*, crustal.usgs.gov/laboratories/icpms/laser\_ablation.html. Accessed Sept. 2017. Web.
- David, C.p. “Heavy Metal Concentrations in Growth Bands of Corals: a Record of Mine Tailings Input through Time (Marinduque Island, Philippines).” *Marine Pollution Bulletin*, vol. 46, no. 2, 2003, pp. 187–196., doi:10.1016/s0025-326x(02)00315-6.
- Dodge, Richard E., and Judith C. Lang. “Environmental correlates of hermatypic coral (*Montastrea annularis*) growth on the East Flower Gardens Bank, northwest Gulf of Mexico1.” *Limnology and Oceanography*, vol. 28, no. 2, 1983, pp. 228–240., doi:10.4319/lo.1983.28.2.0228.
- Fallon, Stewart J., et al. “Porites Corals as Recorders of Mining and Environmental Impacts: Misima Island, Papua New Guinea.” *Geochimica Et Cosmochimica Acta*, vol. 66, no. 1, 2002, pp. 45–62., doi:10.1016/s0016-7037(01)00715-3.
- Fleitmann, Dominik, et al. “East African Soil Erosion Recorded in a 300 Year Old Coral Colony from Kenya.” *Geophysical Research Letters*, vol. 34, no. 4, 2007, doi:10.1029/2006gl028525.
- Gao, Ning. “Radiochemical Analysis by High Sensitivity Micro X-Ray Fluorescence Detection.” Dec. 2006, doi:10.2172/882477.
- Glynn P (1993) Coral reef bleaching: ecological perspectives. *Coral Reefs*, 12, 1–17.
- Goreau, T. J. “Carbon metabolism in calcifying and photosynthetic organisms: theoretical models based on stable isotope data.” *Rosenstiel School of Marine & Atmospheric Science*, vol. 2, 1977, pp. 395–401.
- Guzmán, Héctor M., and Carlos E. Jiménez. “Contamination of coral reefs by heavy metals along the Caribbean coast of Central America (Costa Rica and Panama).” *Marine Pollution Bulletin*, vol. 24, no. 11, 1992, pp. 554–561., doi:10.1016/0025-326x(92)90708-e.
- “How Does XRF Work? - Handheld XRF Analyzer Spectrometer, X-Ray Fluorescence Analyzer, PMI Gun, XRF Scanner Instrument, XRF Tester Device, Portable XRF Analyzer Machine | Bruker.” *Bruker.com*, 30 June 2016, www.bruker.com/products/x-ray-diffraction-and-elemental-analysis/handheld-xrf/how-xrf-works.html. Web.
- Hudson J, Hanson KJ, Halley RB, Kindinger JL (1994) Environmental implications of growth rate changes in *Montastraea annularis*: Biscayne National Park. *Florida Bulletin of Marine Science*, 54, 647–669.



- Jansen, Eystein; Veum, T (1990): Stable isotope analysis of foraminifera from sediment core V23-81 (Table 2). *PANGAEA*, <https://doi.org/10.1594/PANGAEA.106768>.
- Jenner, G.A et al. "ICP-MS - A powerful tool for high-Precision trace-Element analysis in Earth sciences: Evidence from analysis of selected U.S.G.S. reference samples." *Chemical Geology*, Elsevier, 26 Mar. 2003, [www.sciencedirect.com/science/article/pii/000925419090145W](http://www.sciencedirect.com/science/article/pii/000925419090145W). Web.
- Keller, Brian, and Elizabeth Johns. "Strong ocean currents connect geographic regions." [Http://Www.aoml.noaa.gov/](http://www.aoml.noaa.gov/), NOAA, [www.aoml.noaa.gov/outreach/floridaseagrant/pdf\\_files/TropicalConnections\\_StrongOceanCurrentsConnectGeographicAreas\\_KellerJohns.pdf](http://www.aoml.noaa.gov/outreach/floridaseagrant/pdf_files/TropicalConnections_StrongOceanCurrentsConnectGeographicAreas_KellerJohns.pdf). Web.
- Mcculloch, Malcolm, et al. "Coral Record of Increased Sediment Flux to the Inner Great Barrier Reef since European Settlement." *Nature*, vol. 421, no. 6924, 2003, pp. 727–730., doi:10.1038/nature01361.
- Rodriguez, Irene B., et al. "Effects of Trace Metal Concentrations on the Growth of the Coral Endosymbiont *Symbiodinium kawagutii*." *Frontiers in Microbiology*, vol. 7, Aug. 2016, doi:10.3389/fmicb.2016.00082.
- Pilson, Michael. "Arsenate uptake and reduction by *Pocillopora verrucosa*." *Limnology and Oceanography*, vol. 19, no. 2, Mar. 1972, pp. 339–341., doi:10.4319/lo.1974.19.2.0339.
- Sabdon, A. "Heavy Metal Levels and Their Potential Toxic Effect on Coral *Galaxea fascicularis* from Java Sea, Indonesia." *Research Journal of Environmental Sciences*, vol. 3, no. 1, Jan. 2009, pp. 96–102., doi:10.3923/rjes.2009.96.102.
- Sammarco, P. W., et al. "Competitive strategies of soft corals (Coelenterata: Octocorallia): Allelopathic effects on selected scleractinian corals." *Coral Reefs*, vol. 1, no. 3, 1983, pp. 173–178., doi:10.1007/bf00571194.
- Sinclair, Daniel J., et al. "High Resolution Analysis of Trace Elements in Corals by Laser Ablation ICP-MS." *Geochimica Et Cosmochimica Acta*, vol. 62, no. 11, 1998, pp. 1889–1901., doi:10.1016/s0016-7037(98)00112-4.
- Shah, Sofia. "Heavy Metal Accumulation in Scleractinian Corals." *SpringerReference*, doi:10.1007/978-90-481-2639-2\_221.
- Shen, Glen T., and Edward A. Boyle. "Determination of lead, cadmium and other trace metals in annually-Banded corals." *Chemical Geology*, vol. 67, no. 1-2, 1988, pp. 47–62., doi:10.1016/0009-2541(88)90005-8.
- Stafford-Smith, Mg, and Rfg Ormond. "Sediment-Rejection mechanisms of 42 species of Australian scleractinian corals." *Marine and Freshwater Research*, vol. 43, no. 4, 1992, p. 683., doi:10.1071/mf9920683.

Vii, Angel T. Bautista, et al. "A coral  $^{129}\text{I}/^{127}\text{I}$  measurement method using ICP-MS and AMS with carrier addition." *Anal. Methods*, vol. 9, no. 35, 2017, pp. 5181–5188., doi:10.1039/c7ay01458a.

Wallace, K.d., et al. "Comparison of the (Linear) 2f field transmitted with a fully realized two-Dimensional effective apodization and the (Nonlinear) 2f harmonic field." *IEEE Ultrasonics Symposium, 2005.*, 2017, doi:10.1109/ultsym.2005.1603067.